

Structure-properties of small donor-acceptor molecules for homojunction single-material organic solar cells

Supplementary information

Natalia Terenti,^a Gavril-Ionel Giurgi,^{a,b} Andreea Petronela Crişan,^a Cătălin Anghel,^a Alexandra Bogdan,^a
Alexandra Pop,^a Ioan Stroia,^a Anamaria Terec,^a Lorant Szolga,^{a,b} Ion Grosu,^a Jean Roncali,^{a*}

^aBabeş-Bolyai University, Faculty of Chemistry and Chemical Engineering, Department of Chemistry and SOOMCC, Cluj-Napoca, 11 Arany Janos str., 400028, Cluj-Napoca, România

^bOptoelectronics Group, Base of Electronics Department, ETTI, Technical University of Cluj-Napoca, Str. 28 Memorandumului str, Cluj-Napoca, 400114, România

1. General information	1
2. Synthesis and characterization	2
3. Crystallography	15
4. Theoretical calculations	17
5. Characterization of photovoltaic properties	20

1. General Information

All reagents and chemicals from commercial sources were used without further purification. Reactions were carried out under nitrogen atmosphere unless otherwise stated. Solvents were dried and purified using standard techniques. Thin-layer chromatography (TLC) was performed on F254 Silica gel 60 chromatography plates and visualized by UV irradiation at 254 nm. Preparative column chromatography was performed with analytical-grade solvents using silica gel (technical grade, pore size 60 Å) with UV irradiation detection or staining with 2,4-dinitrophenylhydrazine or KMnO_4 solutions. NMR spectra were recorded on a Bruker AVANCE III 400 (^1H , 400 MHz and ^{13}C , 100 MHz). Chemical shifts are given in ppm relative to TMS and coupling constants (J) in Hz. High resolution mass spectra (HRMS) in positive ion mode, using APCI or electrospray ionization mode were recorded with an LTQ XL Orbitrap ThermoScientific mass spectrometer. MALDI-TOF MS spectrum was recorded on Bruker Biflex-IIIITM apparatus, equipped with a 337 nm N₂ laser and exact mass determination on a Spiral-TOF Jeol JMS3000, using a dithranol matrix, in positive mode. UV-vis measurements were performed in CH_2Cl_2 (HPLC grade) at room temperature using a Shimadzu UV spectrophotometer (UV-1800). Melting points were measured using a digital Kleinfeld Apotec melting point apparatus and values are uncorrected. Cyclic voltammetry was performed in DCM solution (HPLC grade). Tetrabutylammoniumhexafluorophosphate (Aldrich) was used without purification. Solutions were purged by argon bubbling prior to each experiment. Experiments were carried out in a one-compartment cell equipped with platinum electrodes and saturated calomel reference electrode (SCE) with a Biologic SP-150 potentiostat with positive feedback compensation

2. Synthesis and characterization

General procedure for compounds 3, 5-8: A solution of the aldehyde (**9, 10, 12**) (0.22 mmol) and corresponding electron-withdrawing moiety (**13-15**) (0.33 mmol) in the appropriate solvent (A: 8 ml dry toluene and 0.3 ml triethylamine; B: 5 ml acetic anhydride; C: 5 ml ethanol) was stirred at 65°C until completion (TLC monitoring). The solvent was removed and the crude product was purified.

(Z)-2-(2-((5-(4-(diphenylamino)phenyl)thiophen-2-yl)methylene)-3-oxo-2,3-dihydro-1H-inden-1-ylidene)malononitrile 3. Method A; purification by precipitating a DCM solution with ethanol. Dark blue solid, *mp* = 264–266°C (dec.), 70 % yield; R_f = 0.62 (Acetone / toluene = 1/50). ¹H NMR (400 MHz, CDCl₃), δ (ppm): 8.86 (s, 1H), 8.69 (dd, J = 1.2 Hz, J = 6.4 Hz, 1H), 7.92 (m, 1H), 7.84 (d, J = 4.4 Hz, 1H), 7.78–7.71 (overlapped peaks, 2H), 7.66 (d, J = 8.8 Hz, 2H), 7.41 (d, J = 4.4 Hz, 1H), 7.34–7.30 (overlapped peaks, 4H), 7.17–7.11 (overlapped peaks, 6H), 7.06 (d, J = 8.8 Hz, 2H). ¹³C NMR (100 MHz, CDCl₃), δ (ppm): 188.5, 161.5, 160.9, 150.1, 147.0, 146.8, 140.1, 138.2, 137.1, 135.7, 135.2, 134.6, 129.7, 127.9, 126.0, 125.7, 125.4, 124.5, 124.0, 123.8, 121.9, 121.8, 114.9, 114.8, 69.2. HRMS (ESI+): *m/z* calcd for C₃₅H₂₁N₃OS: 531.1400 M⁺, found: 531.1379.

(Z)-2-(2-((5-(4-(methyl(phenyl)amino)phenyl)thiophen-2-yl)methylene)-3-oxo-2,3-dihydro-1H-inden-1-ylidene)malononitrile 4. A mixture of carbaldehyde **11** (50 mg, 0.17 mmol) and compound **13** (50 mg, 0.26 mmol) in a 40% V/V solution of toluene in CCl₄ was heated until both reagents were completely solubilized. The solution was cooled down at room temperature and a few drops of pyridine were added. The reaction mixture was stirred under argon atmosphere overnight. The solvent was removed in vacuo and the residue was chromatographed on silica gel (eluent: 2:1 dichloroethane/petroleum ether). Product **4** was additionally washed with petroleum ether and diethyl ether. Dark blue solid, *mp* = 250-251 °C (dec.), 79 % yield; R_f = 0.5 (methylene chloride / petroleum ether = 2 / 1). ¹H NMR (400 MHz, CD₂Cl₂) δ (ppm): 8.82 (s, 1H), 8.66 (d, J = 7.2 Hz, 1 H), 7.84–7.91 (overlapped peaks, 2 H), 7.76 (t, J = 7.2 Hz, 2 H), 7.69 (d, J = 8.4 Hz, 2 H), 7.40–7.42 (overlapped peaks, 3 H), 7.27–7.19 (overlapped peaks, 3 H), 6.88 (d, J = 8.3 Hz, 2 H), 3.40 (s, 3 H). ¹³C NMR (100 MHz, CDCl₃) δ (ppm): 188.6, 162.8, 161.0, 150.9, 147.5, 147.3, 140.1, 138.2, 137.1, 135.2, 135.0, 134.4, 130.0, 128.1, 125.5, 125.3, 123.7, 123.4, 123.1, 121.2, 115.7, 115.1, 115.0, 68.6, 40.5. HRMS (APCI+): *m/z* calcd. for C₃₀H₁₉N₃OS 469.1243 M⁺, found 469.1250.

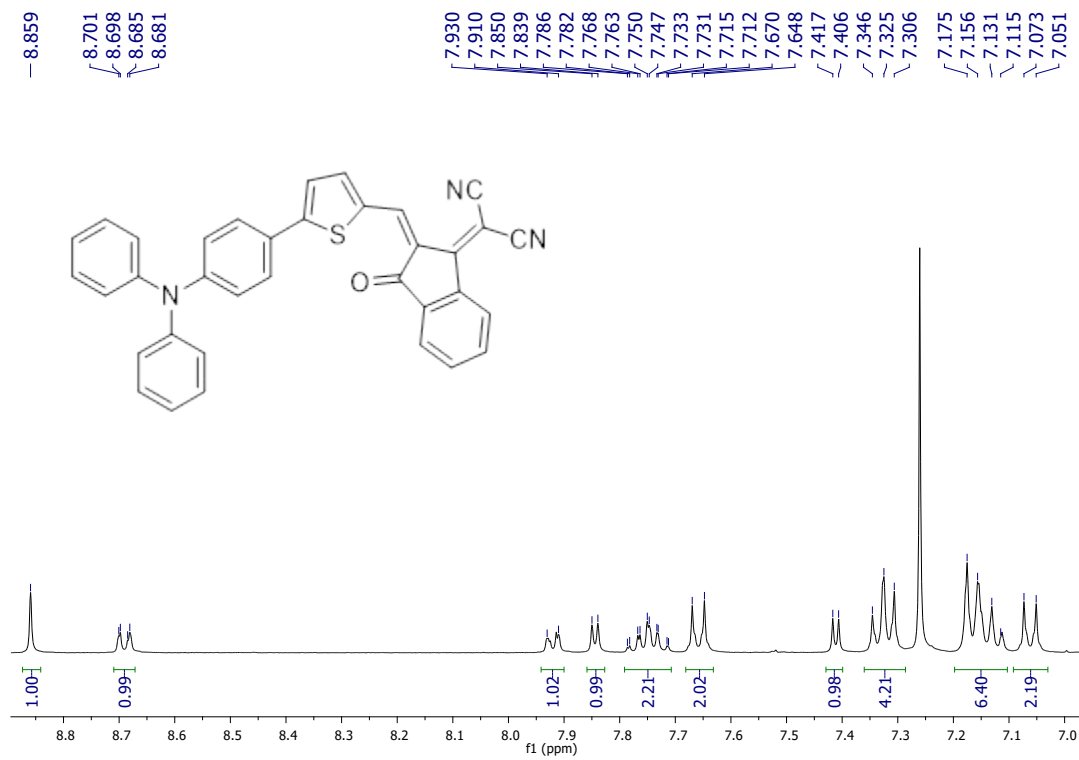
(Z)-2-(2-((5-(4-(naphthalen-2-yl(phenyl)amino)phenyl)thiophen-2-yl)methylene)-3-oxo-2,3-dihydro-1H-inden-1-ylidene)malononitrile 5. Method A; purification by precipitating a DCM solution with ethanol and further washing of the precipitate with ethanol and diethylether. Dark blue solid, *mp* = 284-285°C, 66 % yield; R_f = ¹H NMR (400 MHz, CDCl₃), δ (ppm): 8.85 (s, 1 H), 8.68 (d, J = 8.0 Hz, 1 H), 7.91 (d, J = 6.8 Hz, 1 H), 7.84–7.79 (overlapped peaks, 3 H), 7.75 (m, 2 H), 7.69–7.65 (overlapped peaks, 3 H), 7.55 (d, J = 1.6, 1 H), 7.45–7.41 (overlapped peaks, 3 H), 7.37–7.31 (overlapped peaks, 3 H), 7.21 (d, J = 7.6 Hz, 2 H), 7.17 (d, J = 7.2 Hz, 1 H), 7.12 (d, J = 8.8 Hz, 2 H). ¹³C NMR (100 MHz, CDCl₃), δ (ppm): 188.5, 161.3, 160.8, 149.9, 146.9, 146.8, 144.4, 140.1, 138.2, 137.0, 135.8, 135.2, 134.6, 134.5, 130.9, 129.8, 125.5, 127.9, 127.8, 127.3, 126.7, 126.3, 125.8, 125.4, 125.0, 124.6, 124.0, 123.8, 122.4, 122.3, 121.9, 114.9, 114.8, 69.2. HRMS (APCI): *m/z* calcd for C₃₉H₂₃N₃OS: 581.1556 M⁺, found 582.1663.

(Z)-2-(2-((5-(4-(diphenylamino)phenyl)thiophen-2-yl)methylene)-3-oxo-2,3-dihydro-1H-cyclopenta bnaphthalen-1-ylidene)malononitrile 6. Method A; purification by precipitating a DCM solution with ethanol. Dark blue solid, *mp*

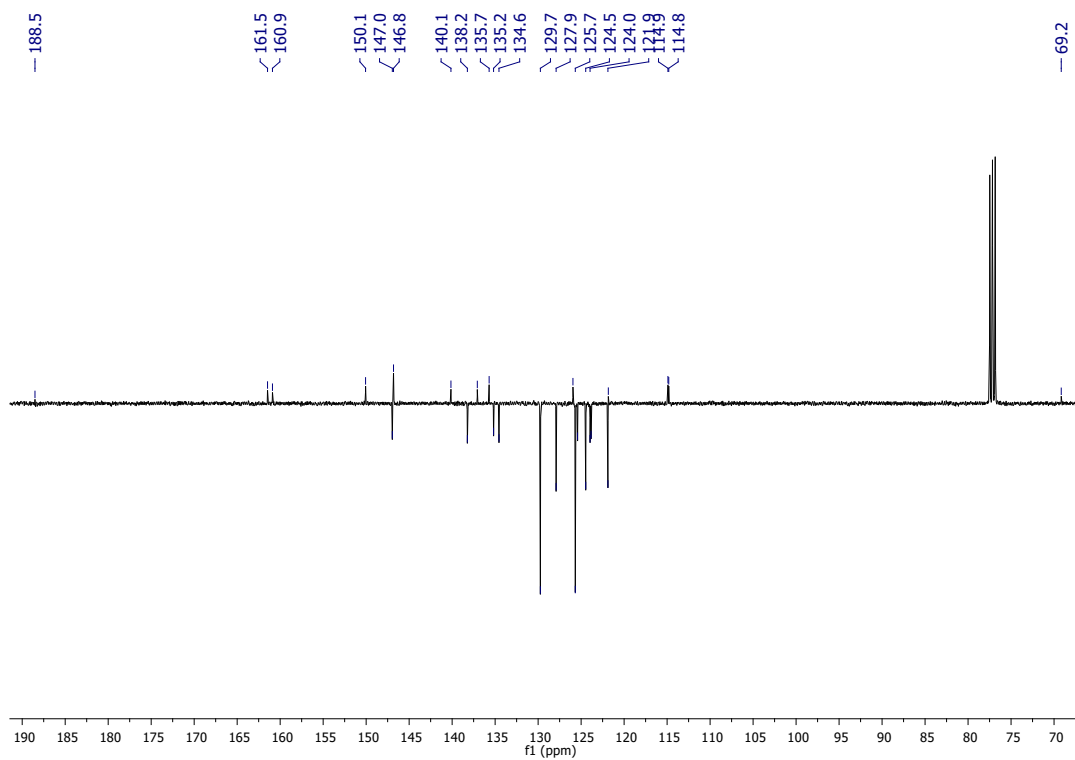
=292–294°C, 68 % yield; R_f = 0.63 (acetone / toluene = 1/50) . **¹H NMR** (400 MHz, CDCl₃), δ (ppm): 9.13 (s, 1H), 8.88 (s, 1H), 8.34 (s, 1H), 8.03 (m, 2H), 7.84 (d, J = 4 Hz, 1H), 7.68–7.64 (overlapped peaks, 4H), 7.40 (d, J = 4 Hz, 1H), 7.33 (m, 4H), 7.18–7.12 (overlapped peaks, 6H), 7.05 (d, J = 8.8 Hz, 2H) . **¹³C NMR** (100 MHz, CDCl₃), δ (ppm): 188.4, 162.2, 160.7, 150.2, 147.5, 146.7, 138.5, 136.3, 136.2, 135.5, 134.9, 133.0, 130.7, 130.3, 129.9, 129.8, 129.7, 128.0, 126.9, 125.8, 125.7, 124.6, 124.2, 123.6, 121.7, 115.5, 115.3, 77.4, 67.7. **HRMS** (ESI⁺): m/z calcd for C₃₉H₂₄N₃O₈: 582.1634 M+H⁺, found 582.1619.

2,2'-(2-((5-(4-(diphenylamino)phenyl)thiophen-2-yl)methylene)-1H-indene-1,3(2H)-diylidene)dimalononitrile 7. Method B; purification by precipitating a DCM solution with hexane and further washing of the precipitate with hexane. Dark blue solid, mp = 247–249°C (dec.), 64 % yield; R_f = 0.50 (acetone / toluene = 1/50) . **¹H NMR** (400 MHz, CDCl₃), δ (ppm): 8.65 (s, 1H), 8.57 (m, 2H), 7.78 (m, 2H), 7.65 (d, J = 4.4 Hz, 1H), 7.52 (d, J = 8.8 Hz, 2H), 7.30–7.34 (overlapped peaks, 5H), 7.17–7.11 (overlapped peaks, 6H), 7.05 (d, J = 8.8 Hz, 2H) . **¹³C NMR** (100 MHz, CDCl₃), δ (ppm): 161.2, 158.1, 150.4, 146.6, 137.4, 136.3, 135.2, 134.7, 129.8, 127.9, 126.6, 126.5, 125.8, 125.7, 125.0, 124.7, 124.3, 122.1, 121.6, 113.7, 113.6. **HRMS** (ESI⁺): m/z calcd for C₃₈H₂₁N₅S 579.1512 M⁺, found 579.1490.

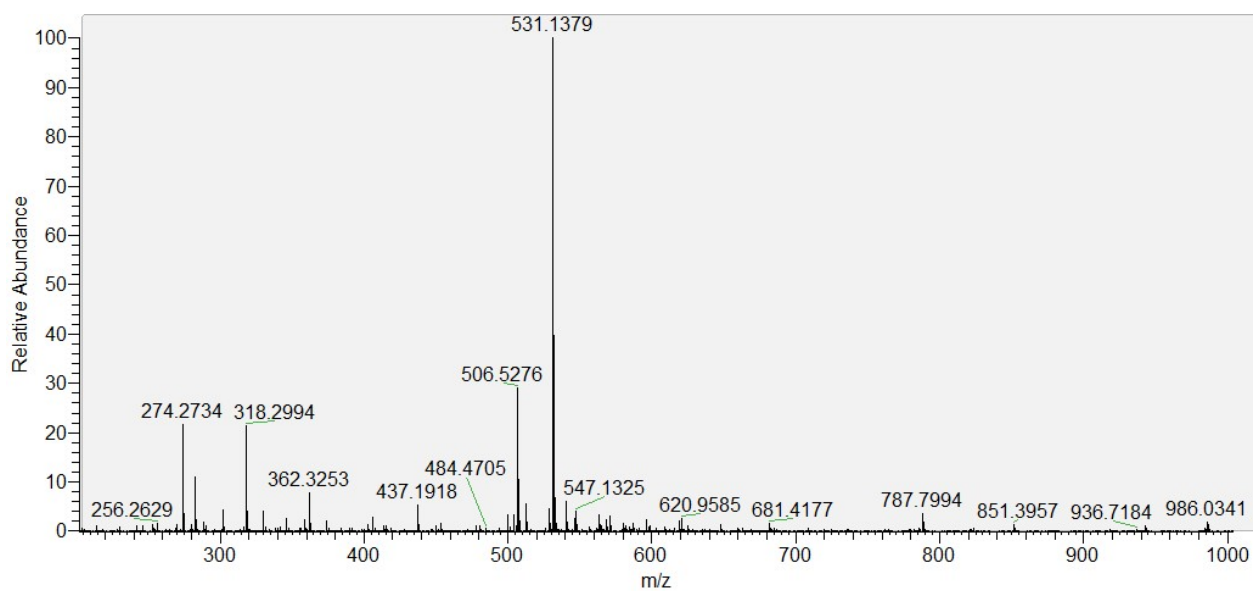
(Z)-2-(2-((4'-(diphenylamino)-1,1'-biphenyl-4-yl)methylene)-3-oxo-2,3-dihydro-1H-inden-1-ylidene)malononitrile 8. Method C; purification by precipitating a DCM solution with ethanol and further washing of the precipitate with ethanol. Dark blue solid, mp = 240–242°C (dec.), 52 % yield; R_f = 0.59 (acetone / toluene = 1/50). **¹H NMR** (400 MHz, CDCl₃), δ (ppm): 8.72 (d, J = 7.6 Hz, 1 H), 8.63 (s, 1 H), 8.27 (d, J = 8.4 Hz, 2 H), 7.96 (d, J = 6.4 Hz, 2 H), 7.85–7.77 (overlapped signals, 2 H), 7.72 (d, J = 8.4 Hz, 2 H), 7.57 (d, J = 8.8 Hz, 2 H), 7.32–7.28 (overlapped signals, 5 H), 7.17–7.13 (overlapped signals, 5 H), 7.08 (m, 2 H). **¹³C NMR** (100 MHz, CDCl₃), δ (ppm): 186.7, 162.1, 148.7, 147.7, 147.4, 145.9, 139.9, 137.6, 135.7, 135.3, 135.1, 132.6, 131.0, 129.6, 129.1, 128.1, 126.4, 125.5, 125.2, 124.5, 123.8, 123.0, 114.4, 114.0, 68.2. **HRMS** (APCI⁺): m/z calcd for C₃₇H₂₄N₃O: 526.1914 M+H⁺, found 526.1888.



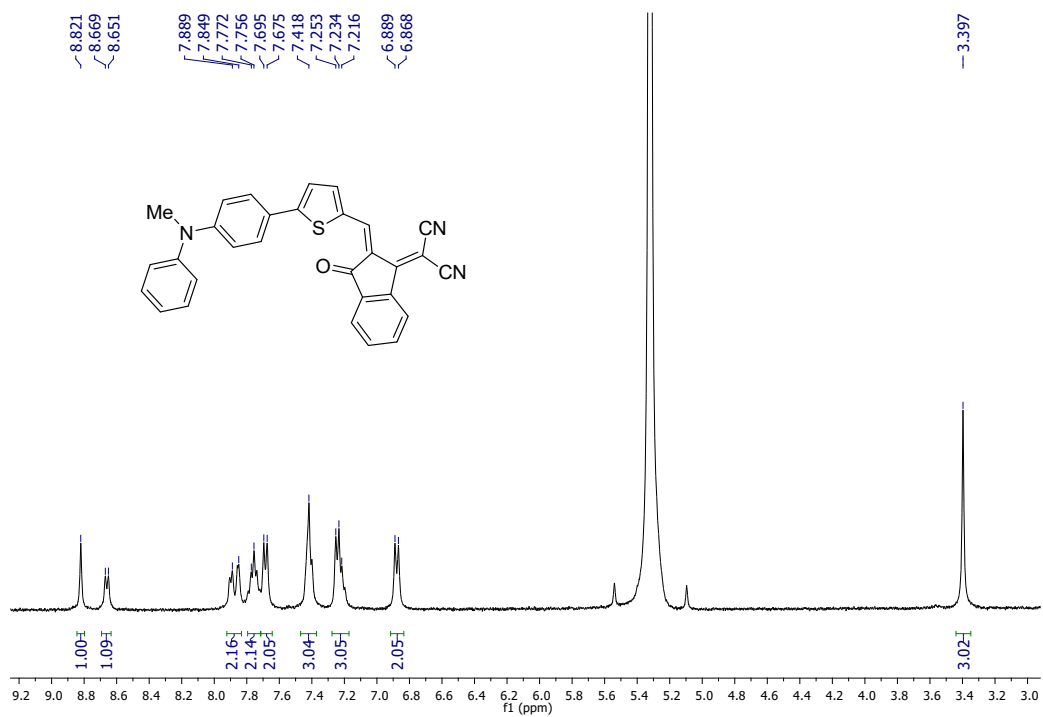
$^1\text{H NMR}$ (400 MHz, CDCl_3) spectrum of **3**



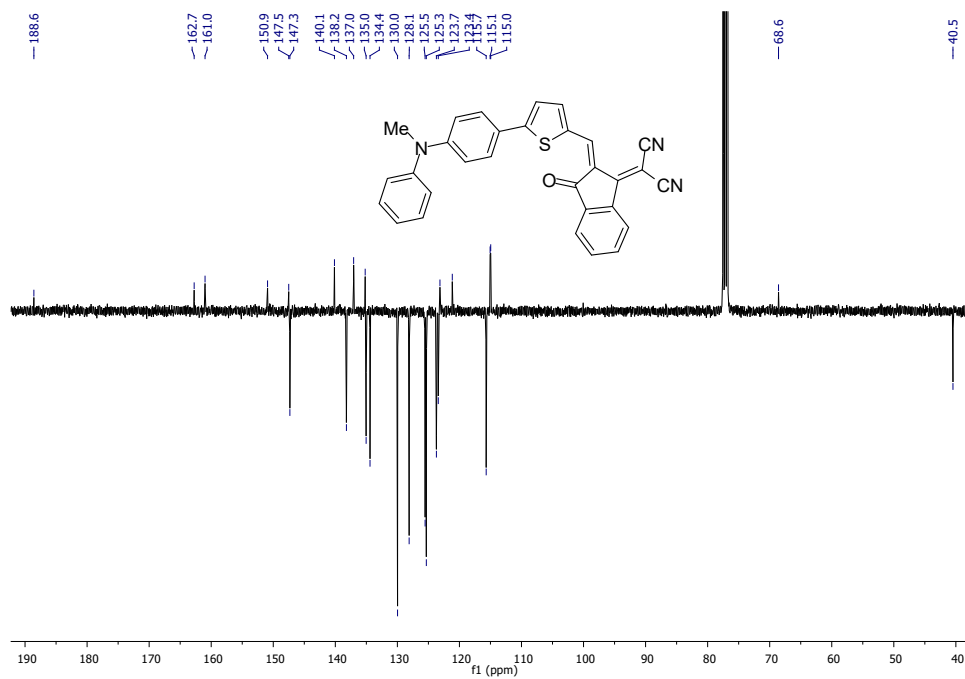
^{13}C (APT) NMR (100 MHz, CDCl_3) spectrum of **3**



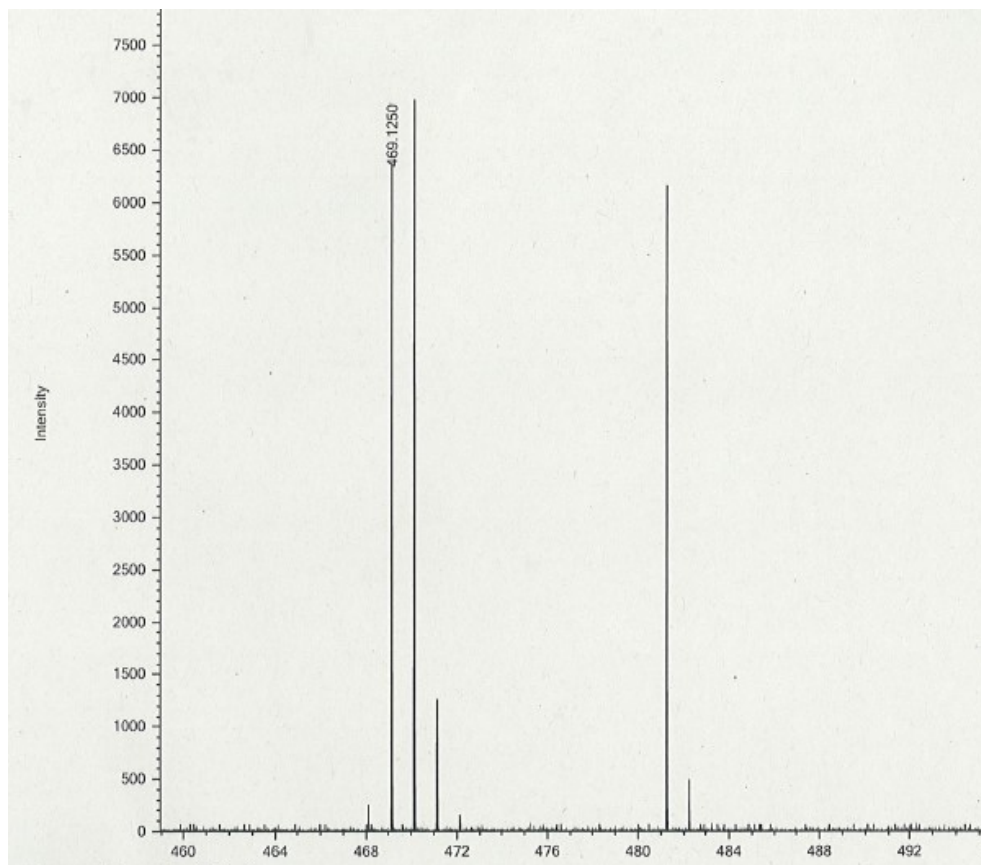
Fragment of ESI(+)-HRMS spectrum of **3**



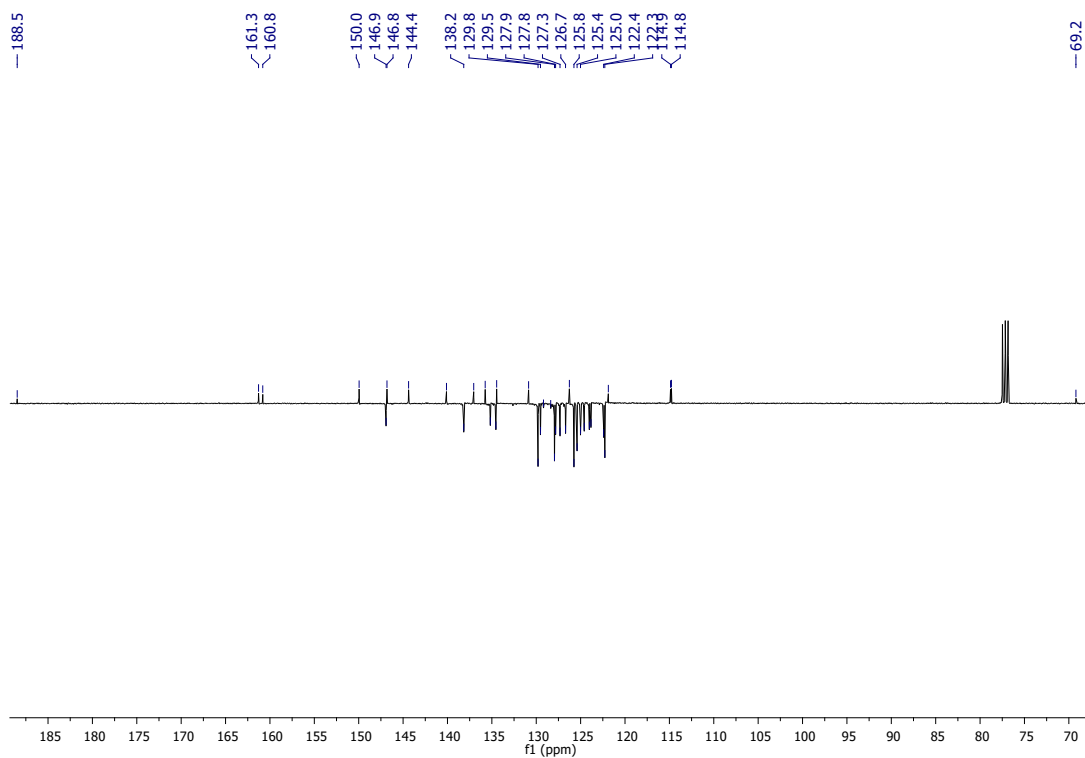
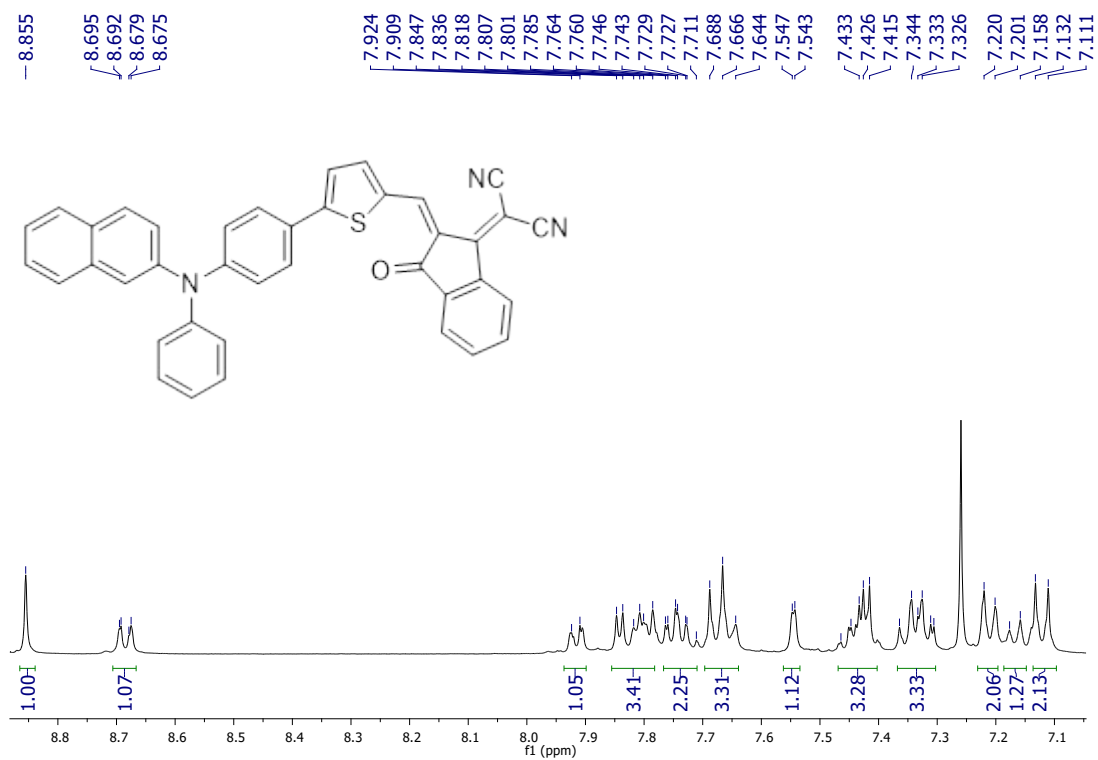
¹H NMR (400 MHz, CD₂Cl₂) spectrum of 4



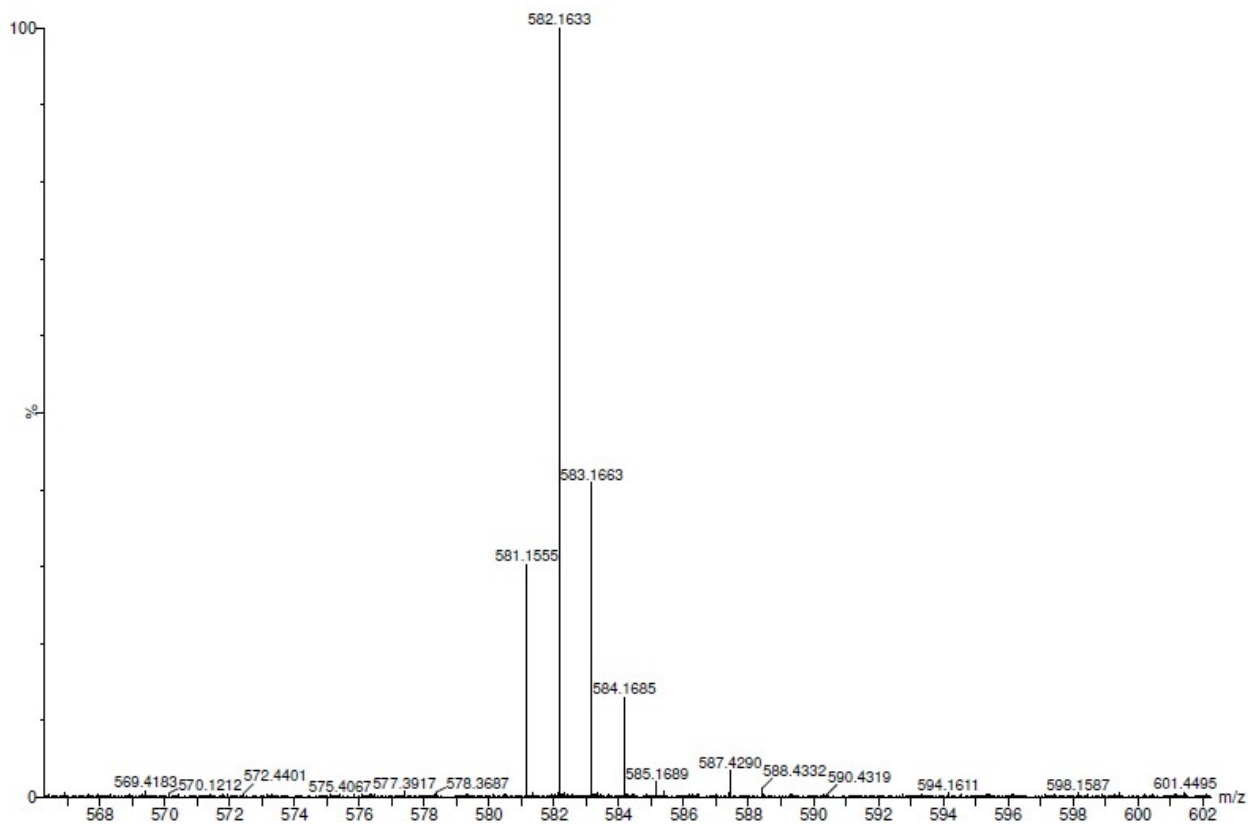
¹³C (APT) NMR (100 MHz, CDCl₃) spectrum of 4



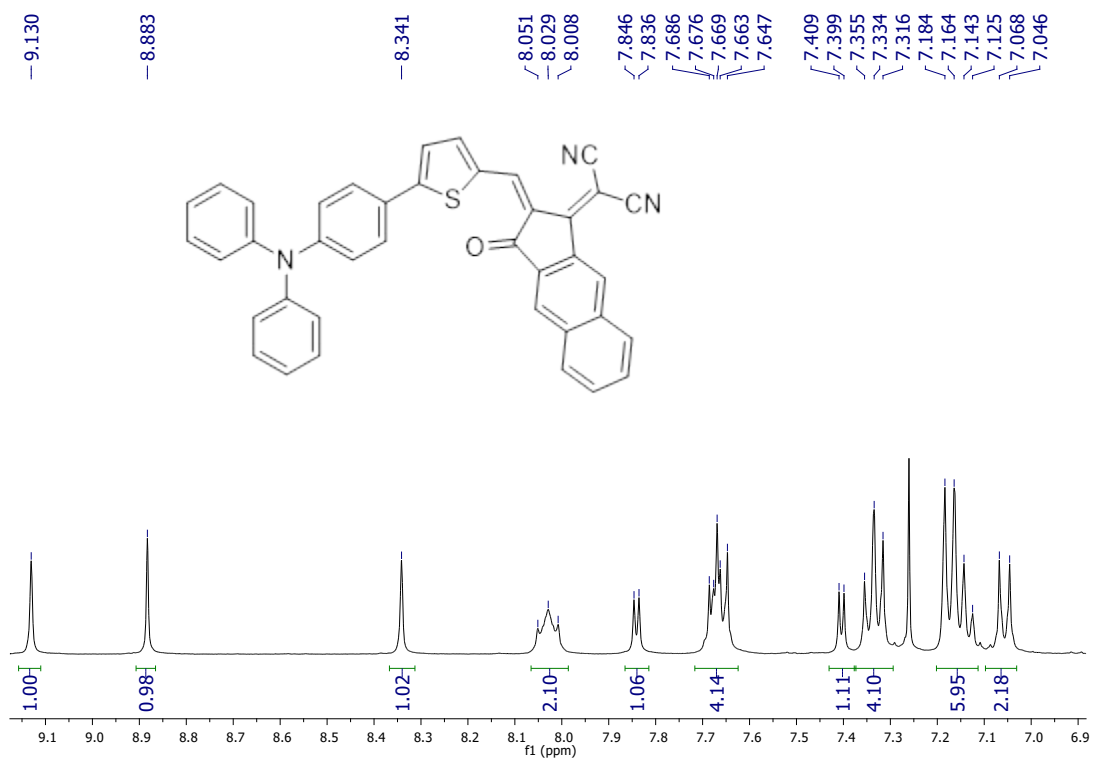
Fragment of MALDI(+)-HRMS spectrum of **4**



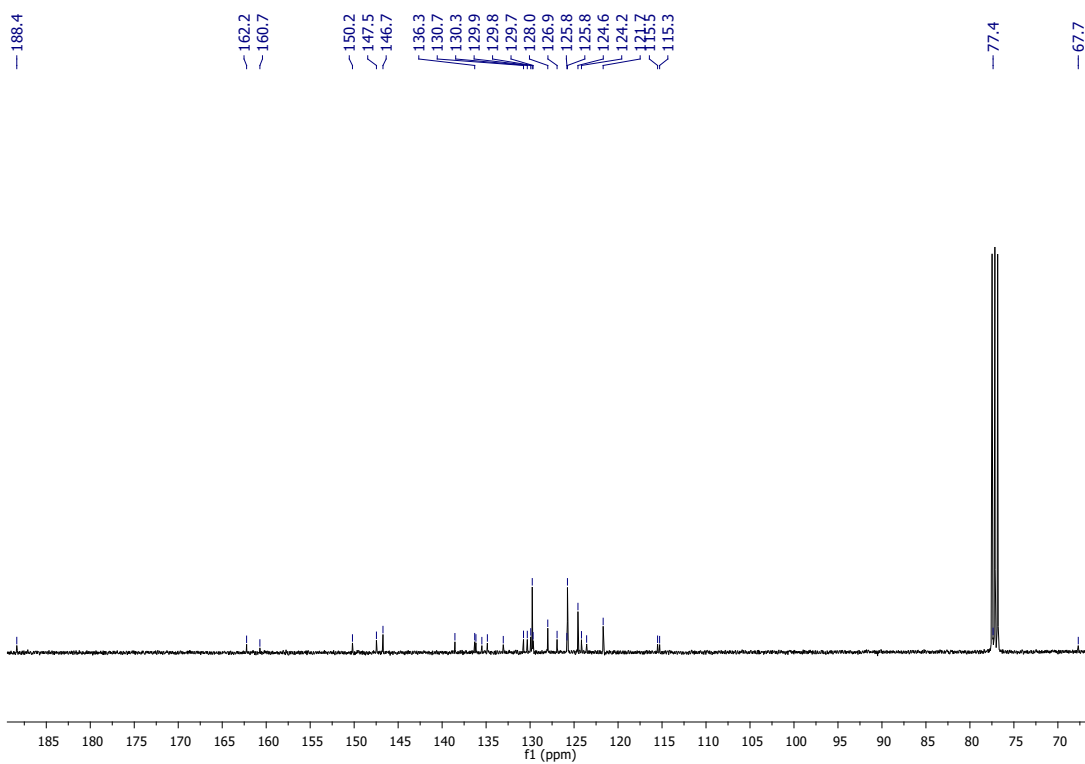
¹³C (APT) NMR (100 MHz, CDCl₃) spectrum of 5



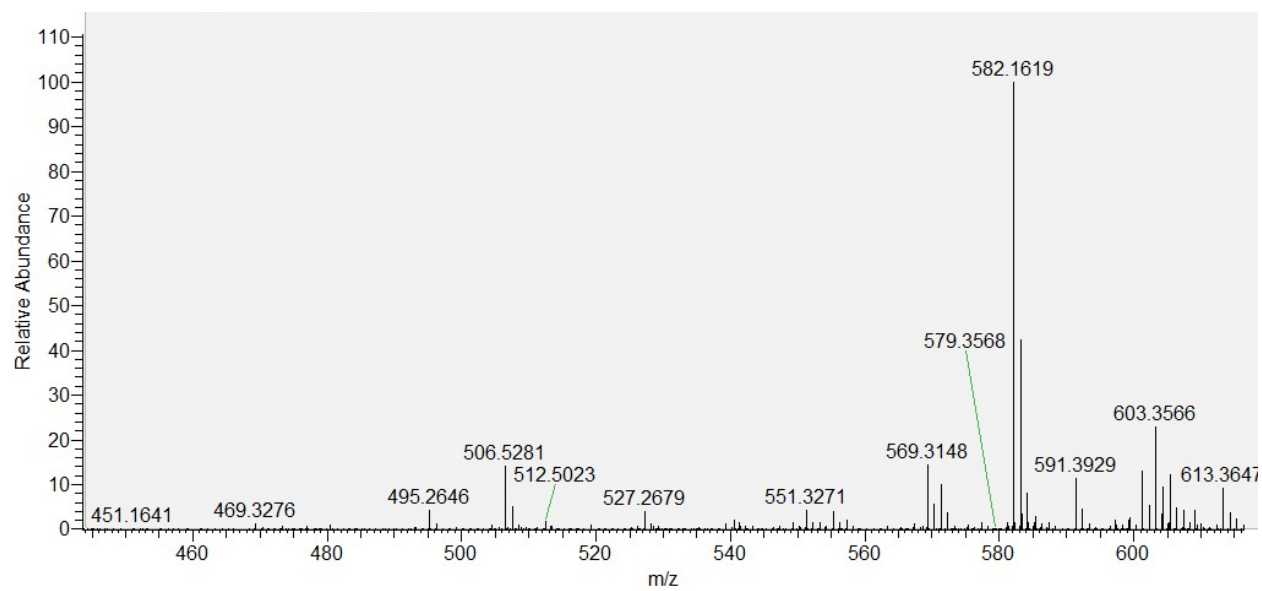
Fragment of ESI(+)-HRMS spectrum of 5

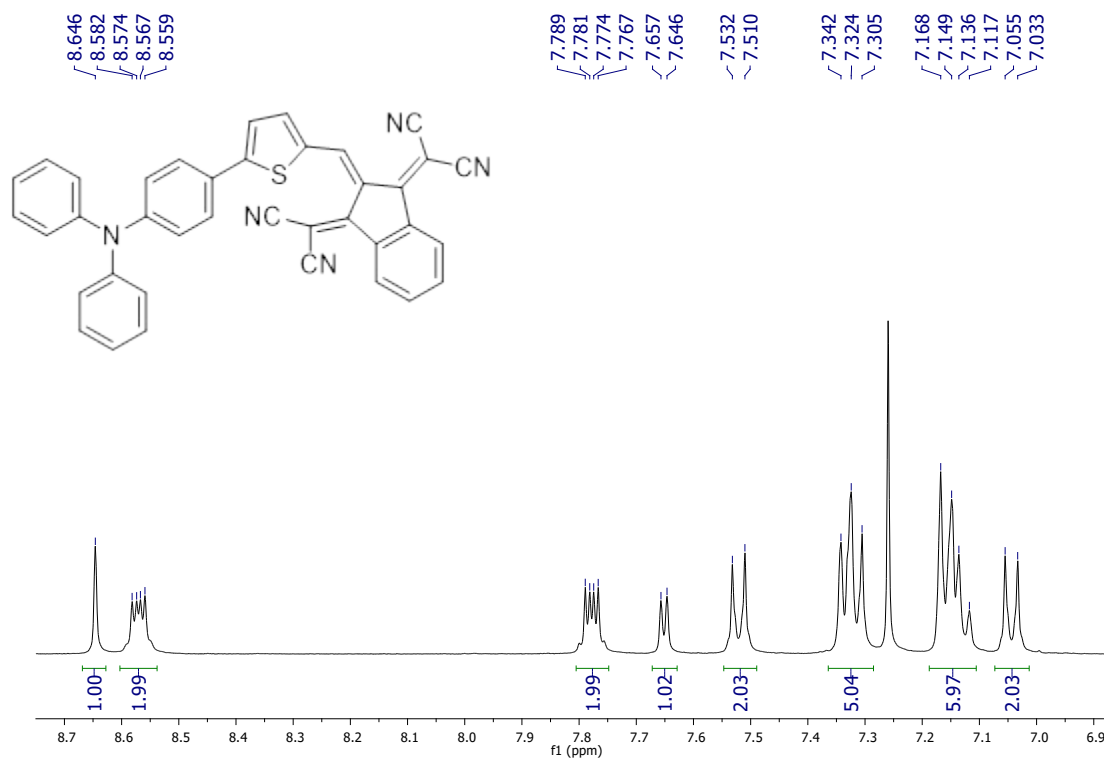


^1H NMR (400 MHz, CDCl_3) spectrum of **6**

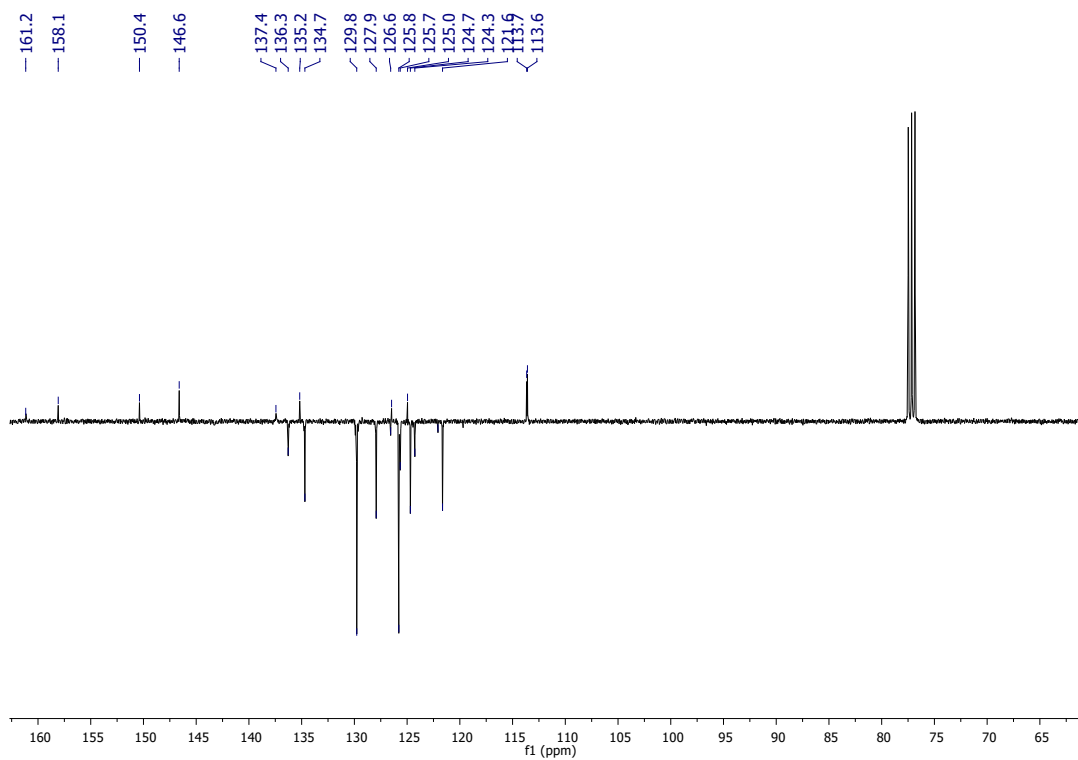


^{13}C NMR (100 MHz, CDCl_3) spectrum of **6**

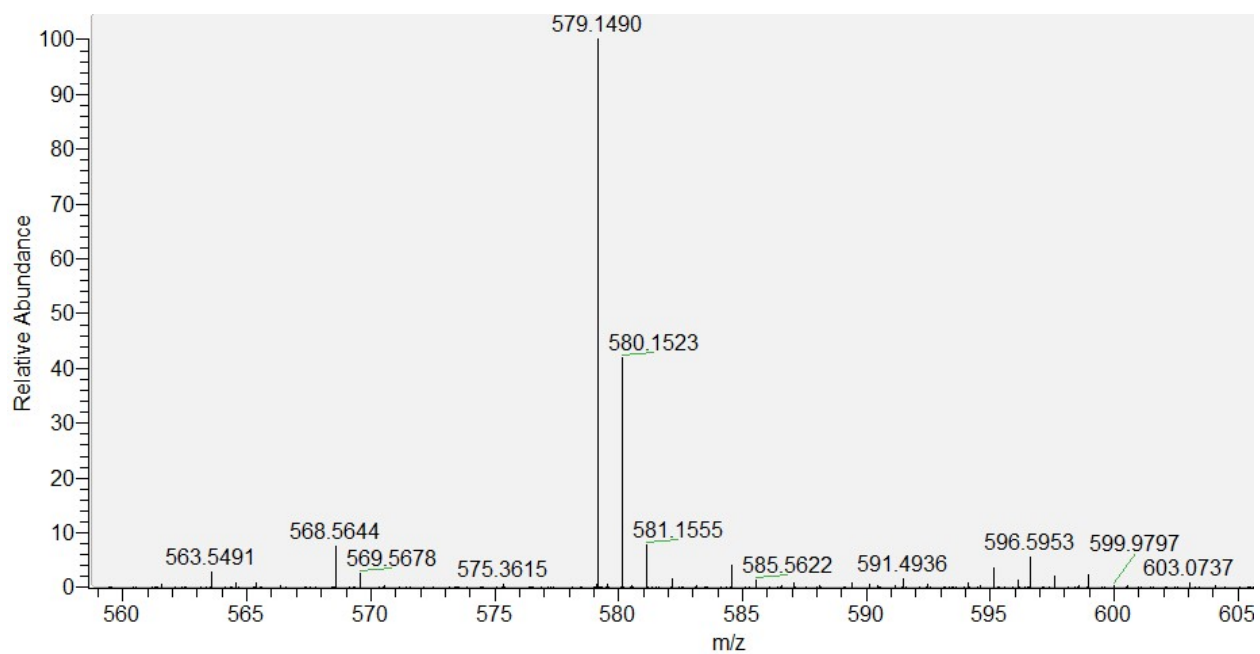




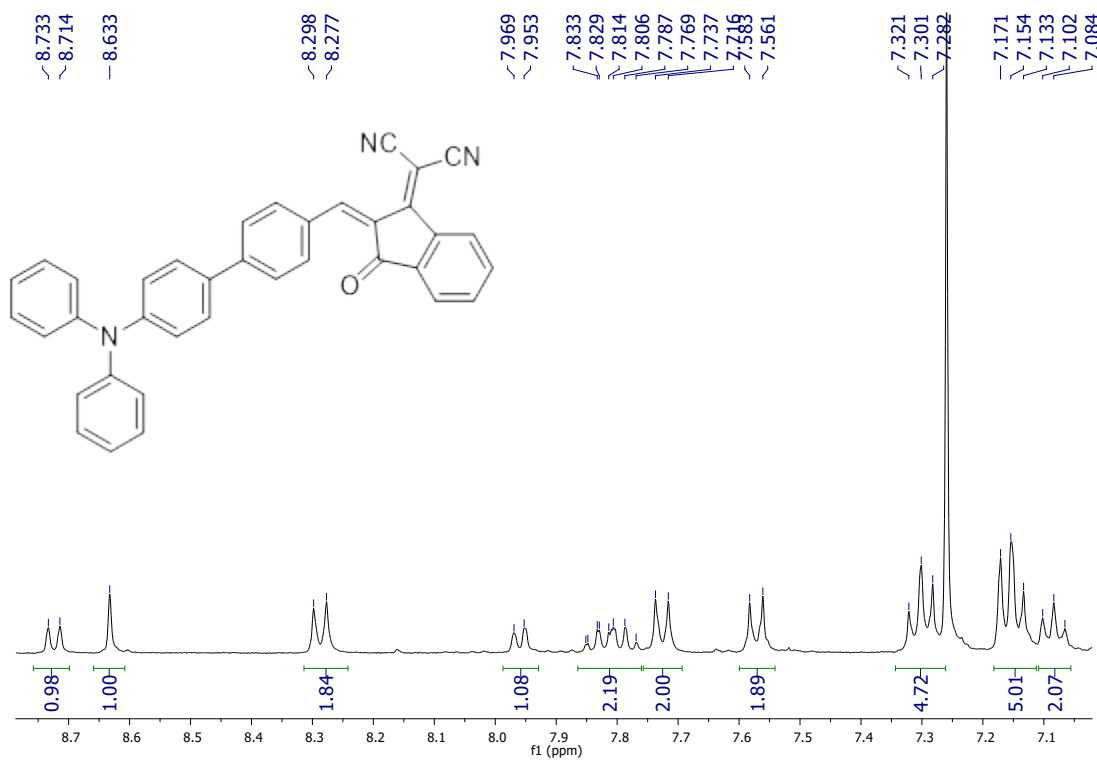
¹H NMR (400 MHz, CDCl₃) spectrum of **7**



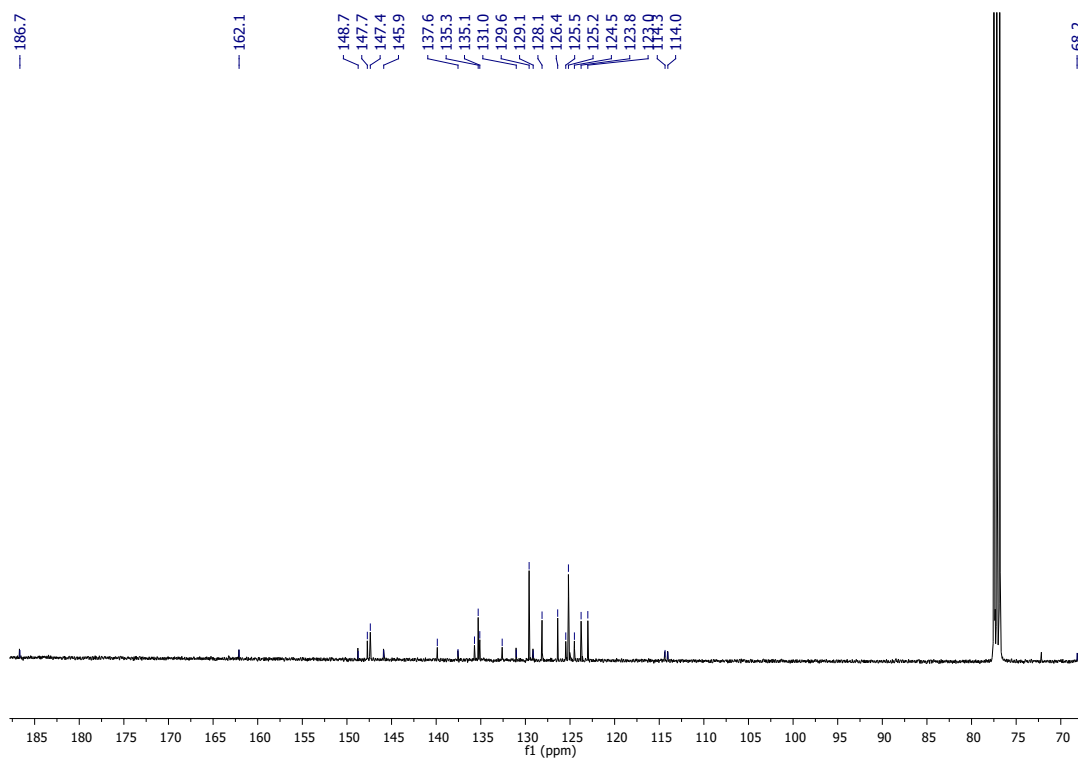
¹³C (APT) NMR (100 MHz, CDCl₃) spectrum of **7**



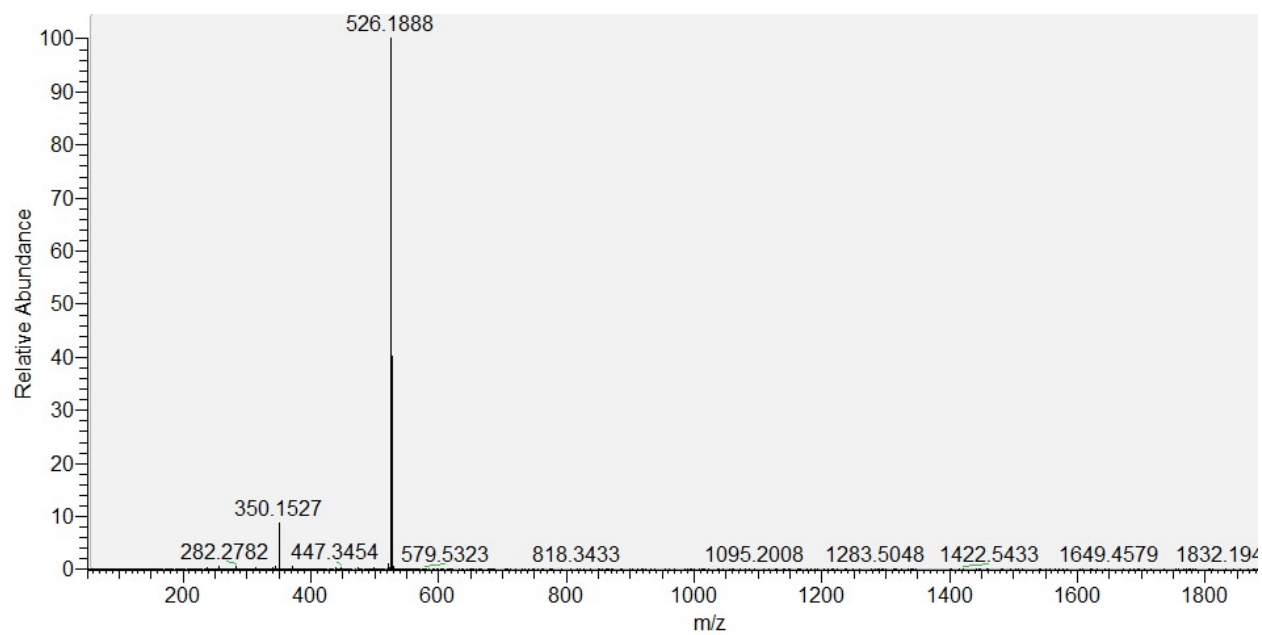
Fragment of ESI(+)-HRMS spectrum of **7**



¹H NMR (400 MHz, CDCl₃) spectrum of **8**



¹³C NMR (100 MHz, CDCl₃) spectrum of **8**



APCI (+)-HRMS spectrum of **8**

3. Crystallography

The crystals of **6** – **8** were mounted on MiTeGen microMounts cryoloops and data were collected on a Bruker D8 VENTURE diffractometer using Mo-K α radiation ($\lambda = 0.71073 \text{ \AA}$) from a I μ S 3.0 microfocus source with multilayer optics, at low temperature (100 K). The structures were refined with anisotropic thermal parameters for non-H atoms. Hydrogen atoms were placed in fixed, idealized positions and refined with a riding model and a mutual isotropic thermal parameter. For structure solving and refinement the Bruker APEX3 Software Packages were used.¹

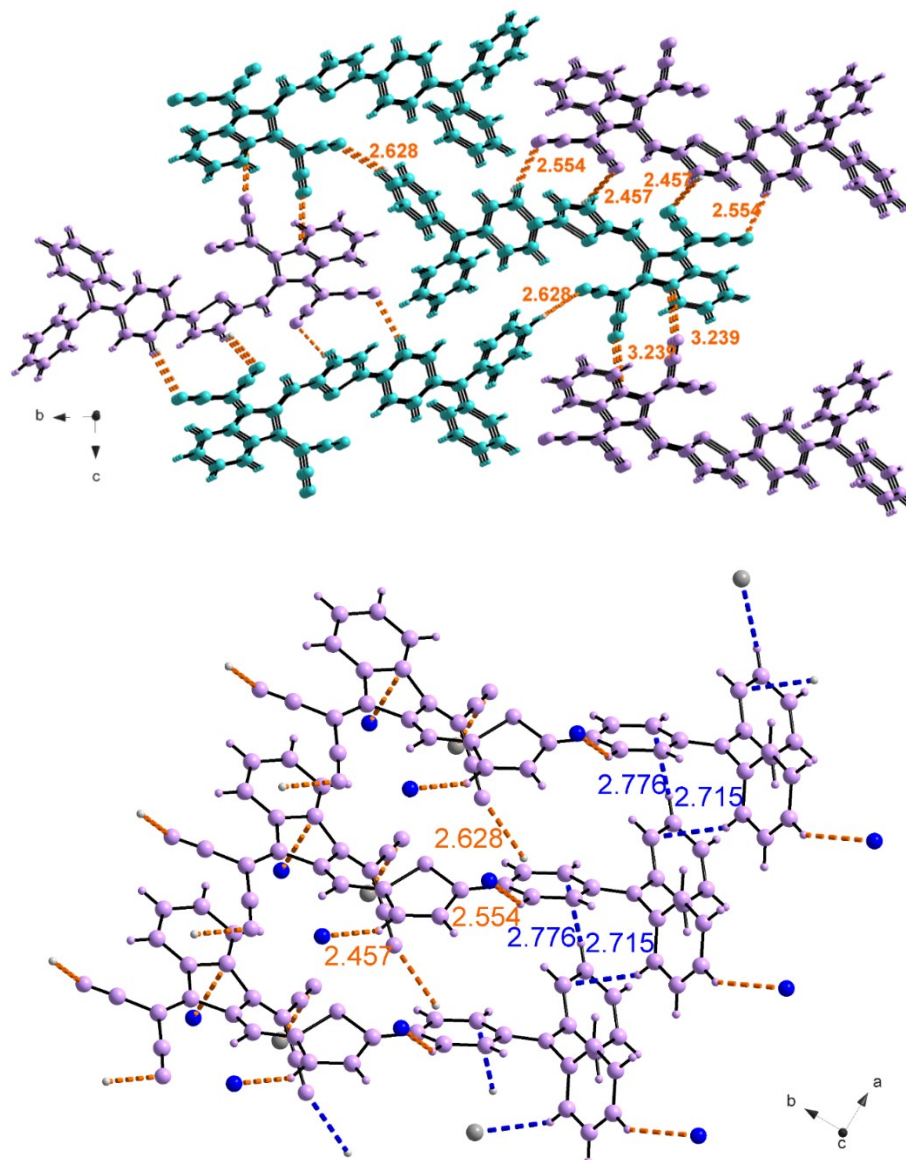


Fig. S1. Top: Ball and stick representation of a fragment of the lattice of **7** displaying the N \cdots H contacts leading to the formation of a 2-D sheet in orange. Two different colors were used to highlight the formation of a 2-D sheets. Bottom: Ball and stick representation of a fragment of the lattice presenting the identified intermolecular contacts (inter-sheet C \cdots H contacts in blue).

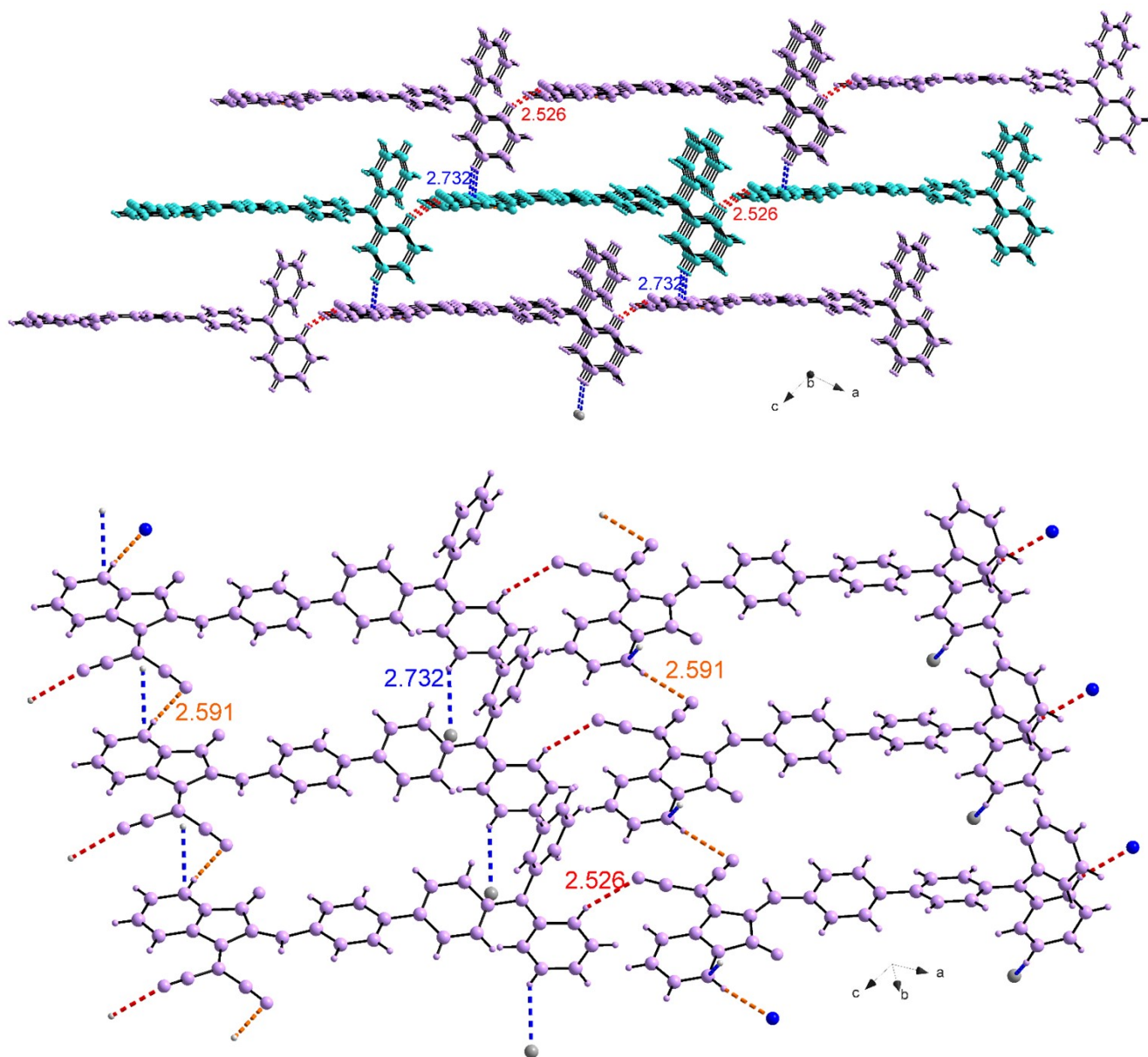


Fig. S2. Top: Ball and stick representation of a fragment of the lattice of **8** presenting the identified intermolecular contacts (inter-sheet C...H contacts in blue and 2-D sheet formation via N...H contacts in red and orange, respectively). Two different colors were used to highlight the 2-D sheets. **Bottom** Ball and stick representation of a fragment of the lattice displaying the N...H contacts leading to the formation of a 2-D sheet.

Table S1. Crystal data and structure refinement for **6** – **8**.

	6	7	8
Empirical formula	C _{39.50} H ₂₄ ClN ₃ OS	C ₃₈ H ₂₁ N ₅ S	C ₃₇ H ₂₃ N ₃ O
Formula weight	624.13	579.66	525.58
Temperature	100(2) K	107(2) K	100(2) K
Wavelength	0.71073 Å	0.71073 Å	0.71073 Å
Crystal system	Monoclinic	Monoclinic	Monoclinic
Space group	C 2/c	P 21/c	C 12/c1
Unit cell dimensions	a = 34.6235(15) Å $\alpha = 90^\circ$ b = 10.2089(4) Å $\beta = 103.9300(10)^\circ$ c = 17.6071(7) Å $\gamma = 90^\circ$	a = 5.5735(4) Å $\alpha = 90^\circ$ b = 35.775(3) Å $\beta = 98.774(2)^\circ$ c = 14.6434(11) Å $\gamma = 90^\circ$	a = 29.6907(9) Å $\alpha = 90^\circ$ b = 9.6237(3) Å $\beta = 106.950(2)^\circ$ c = 19.2394(5) Å $\gamma = 90^\circ$
Volume	6040.5(4) Å ³	2885.6(4) Å ³	5258.6(3) Å ³
Z	8	4	8
Density (calculated)	1.373 mg/m ³	1.334 mg/m ³	1.328 g/m ³
Absorption coefficient	0.234 mm ⁻¹	0.150 mm ⁻¹	0.081 mm ⁻¹
F(000)	2584	1200	2192
Crystal size mm ³	0.150 x 0.089 x 0.017	0.132 x 0.072 x 0.012	0.060 x 0.075 x 0.092
Theta range for data	2.085 to 28.294°.	2.213 to 25.000°.	2.21 to 28.29°
collection Index ranges	-46<=h<=46, -13<=k<=13, -20<=l<=23	-6<=h<=5, -42<=k<=42, -17<=l<=17	-39<=h<=39, -12<=k<=12, -25<=l<=25
Reflections collected	76339	26311	158412
Independent reflections	7505 [R(int) = 0.0996]	5087 [R(int) = 0.1577]	6540 [R(int) = 0.0631]
Completeness to $\theta = 25^\circ$	100.0 %	99.8 %	100.0 %
Refinement method	Full-matrix least-squares on		
Data/restraints/parameters	7505 / 0 / 411	5087 / 0 / 1456	6540 / 0 / 370
Goodness-of-fit on F ²	1.026	3.608	1.036
Final R indices [I>2 σ (I)]	R1 = 0.0459, wR2 = 0.0904	R1 = 0.1337, wR2 = 0.3479	R1 = 0.0424, wR2 = 0.1001
R indices (all data)	R1 = 0.0834, wR2 = 0.1058	R1 = 0.2318, wR2 = 0.3648	R1 = 0.0573, wR2 = 0.1109
Largest diff. peak and hole	0.283 and -0.426 e.Å ⁻³	2.416 and -1.717 e.Å ⁻³	0.301 and -0.237 e.Å ⁻³

4. Theoretical calculations

DFT computational study was performed using Gaussian 09 package,² employing the dispersion corrected form of B3LYP exchange-correlation functional (B3LYP-D3, with D3 standing for Grimme's dispersion corrections)³ and Def2-TZVP as basis set.^{4,5} All geometries were fully optimized in DCM as solvent (using default SCRF method) without any symmetry constraints.

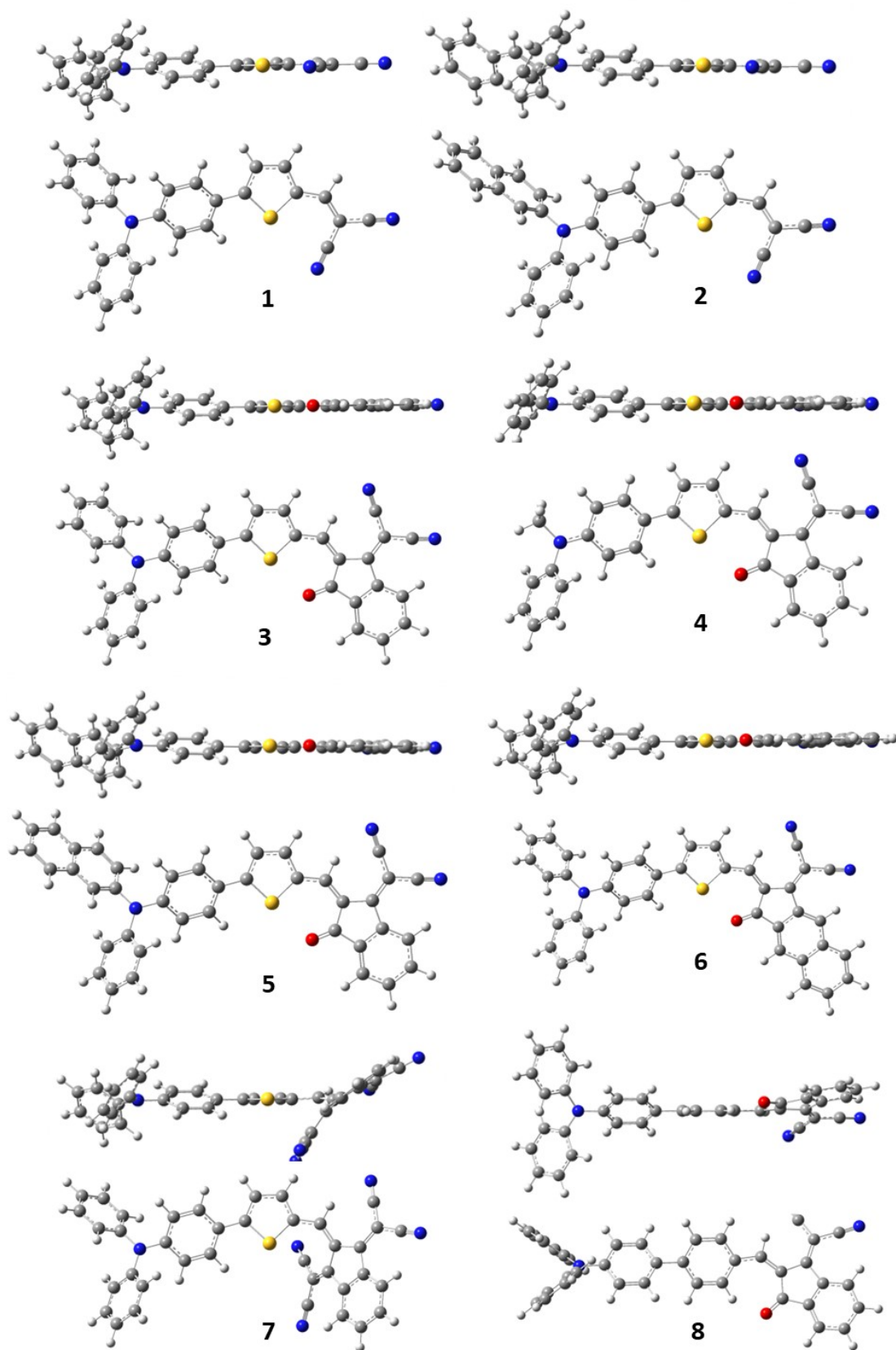


Fig. S3. Optimized ground state geometries of compounds 1-8.

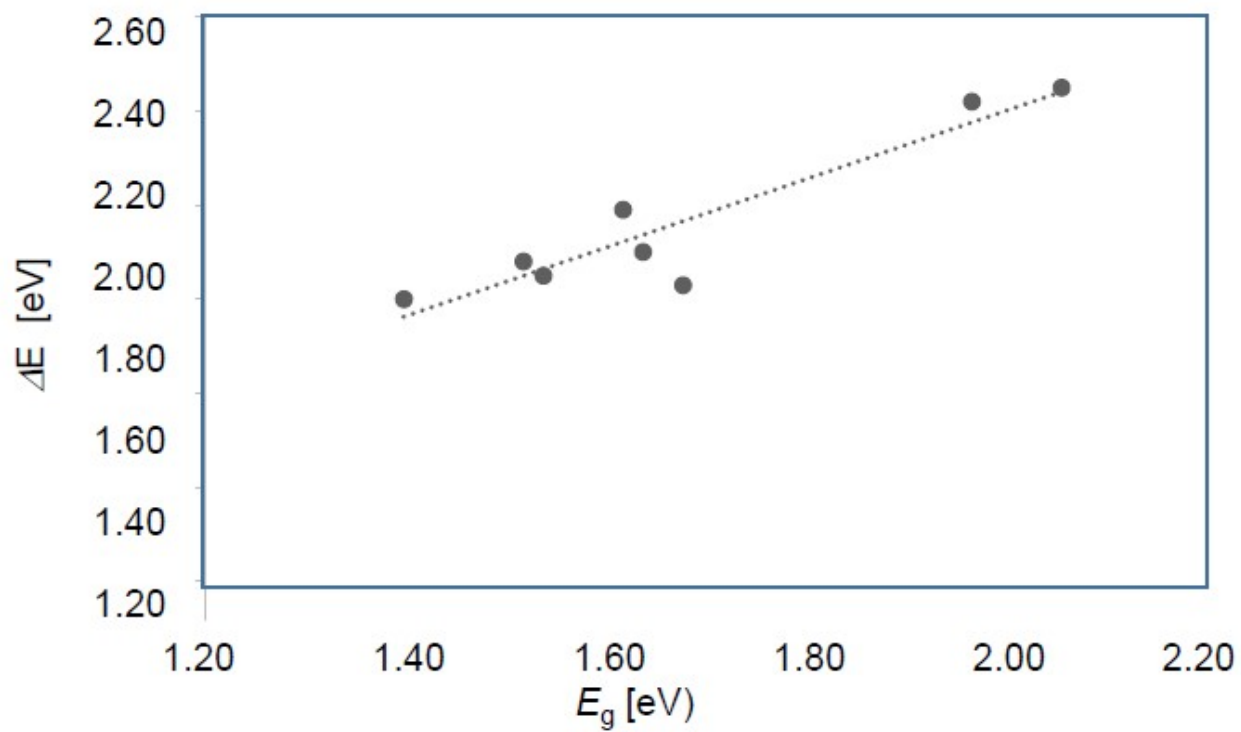


Fig. S4. correlation between the calculated ΔE and experimental E_g values

5. Characterization of photovoltaic properties

The photovoltaic performances of the molecules were evaluated on 28 mm² active area cells of direct and inverted structures. Indium-tin oxide (ITO) coated glass slides of 24 × 25 × 1.1 mm with a sheet resistance of $RS = 7 \Omega/\text{sq}$ were purchased from Praezisions Glas & Optik GmbH. The ITO layer was patterned by a 37% hydrochloric acid solution and zinc powder etching. The substrates were then washed with a diluted Deconex® 12 PA-x solution (2% in water) and scrubbed using dish washing soap before being cleaned by a series of ultrasonic treatments for 15 min in distilled water, acetone and isopropanol. Once dried under a steam of nitrogen, a UV-ozone plasma treatment (UV/Ozone ProCleaner Plus, Bioforce Nanosciences) was performed for 15 min. For cell with inverted structure, a ZnO layer (40 nm) was deposited from a solution of 198 mg of zinc acetate and 0.54 mL of ethanolamine in 6 mL of ethanol. The solution was stirred at 100 °C for 12 h, spin-cast on ITO substrates and thermally annealed at 200 °C for 1 h. The device was then completed by successive thermal evaporation a pressure of 1.5×10^{-6} Torr of the active molecule (20 nm), MoO₃ (16 nm) and aluminium (100 nm) through a shadow mask defining two cells of 28 mm² on each ITO substrate. Cells of direct structure were fabricated by successive thermal evaporation of MoO₃ (10 nm) active molecule (20nm) BPhen (8nm) and aluminium (100 nm). $J_{vs} V$ curves were recorded in the dark and under illumination using a Keithley 236 source-measure unit and a home-made acquisition program. The light source is an AM1.5 Solar Constant 575 PV simulator (Steuernagel Lichttechnik, equipped with a metal halogen lamp). The light intensity was measured by a broad-band power meter (13PEM001, Melles Griot). EQE was measured under ambient atmosphere using a halogen lamp (Osram) with an Action Spectra Pro 150 monochromator, a lock-in amplifier (Perkin Elmer 7225 and a Hamamatsu S2281 photodiode).

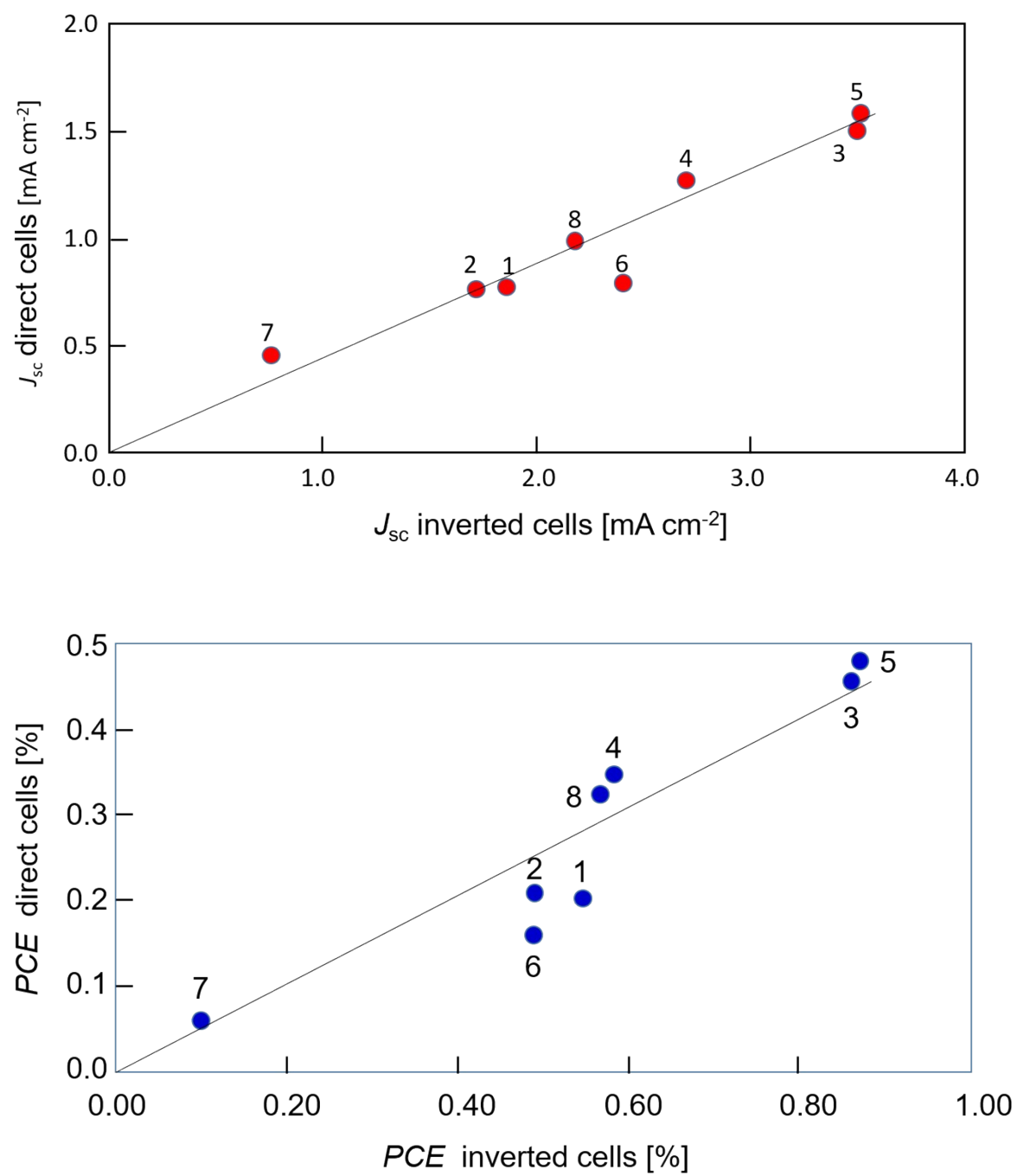


Fig. S5. Correlation between J_{sc} and PCE values of direct and inverted cells

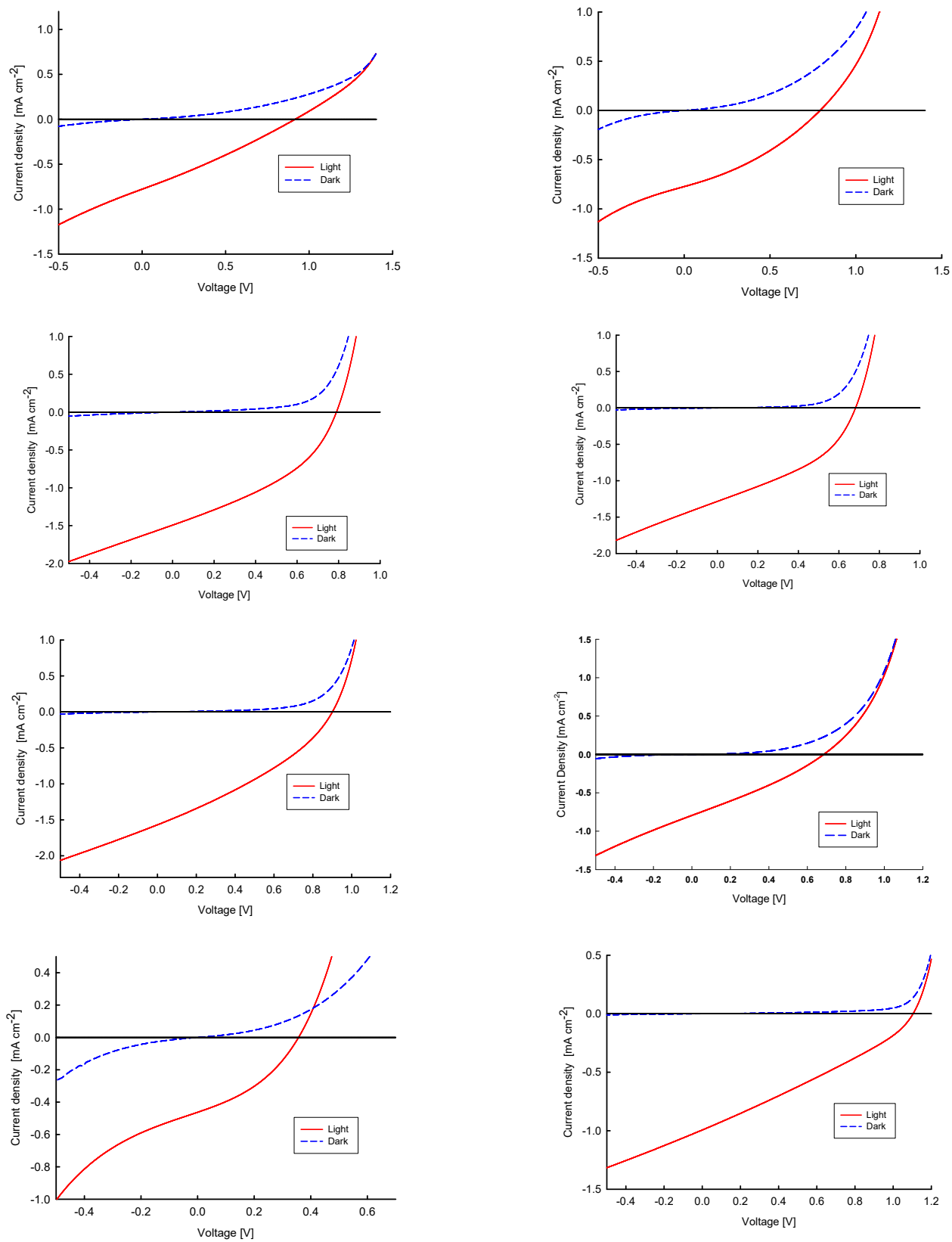


Fig. S6. J vs V curves for direct cells under AM 1.5 simulated solar light.

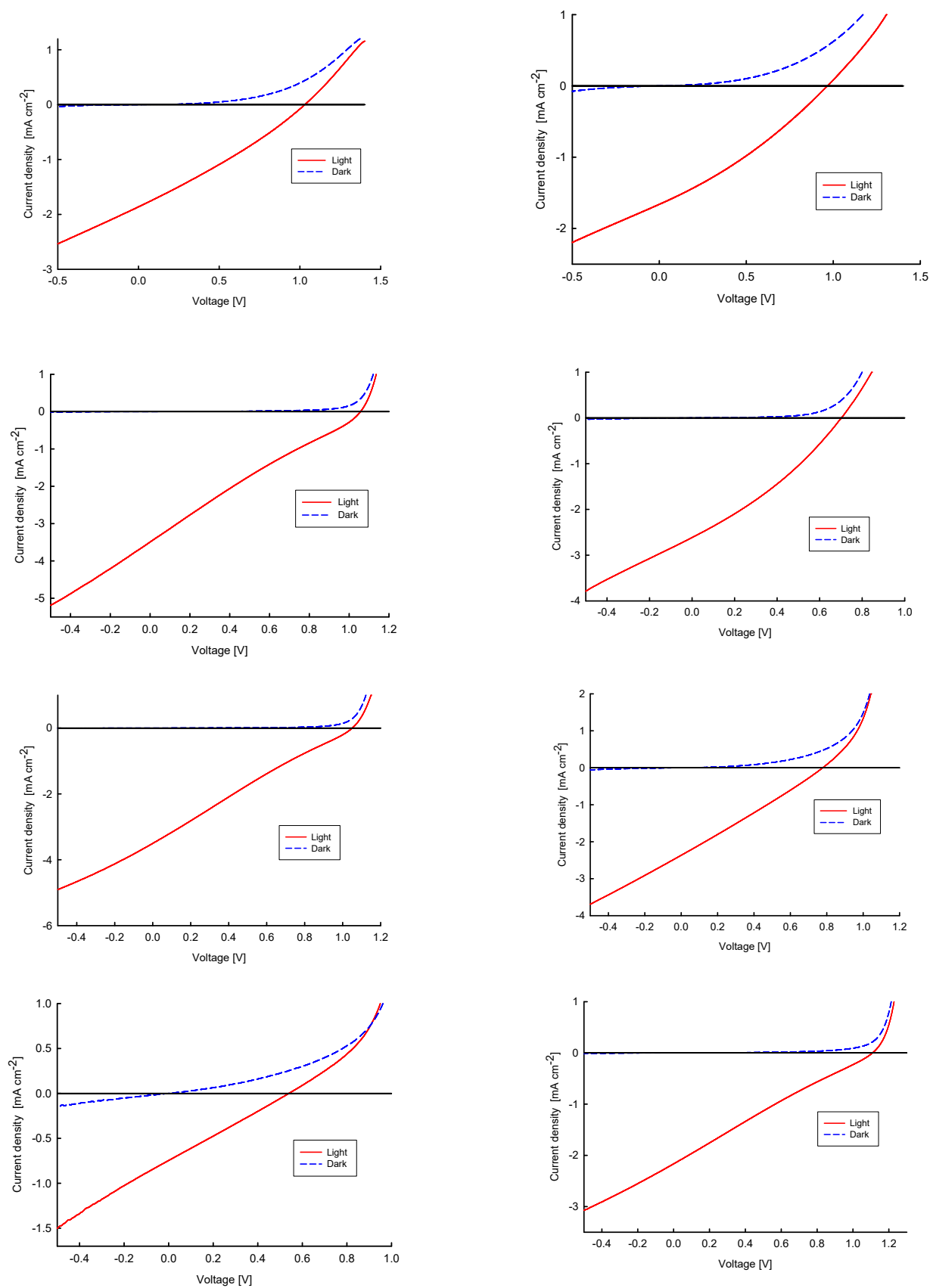


Fig. S7. J vs V curves for inverted cells under AM 1.5 simulated solar light

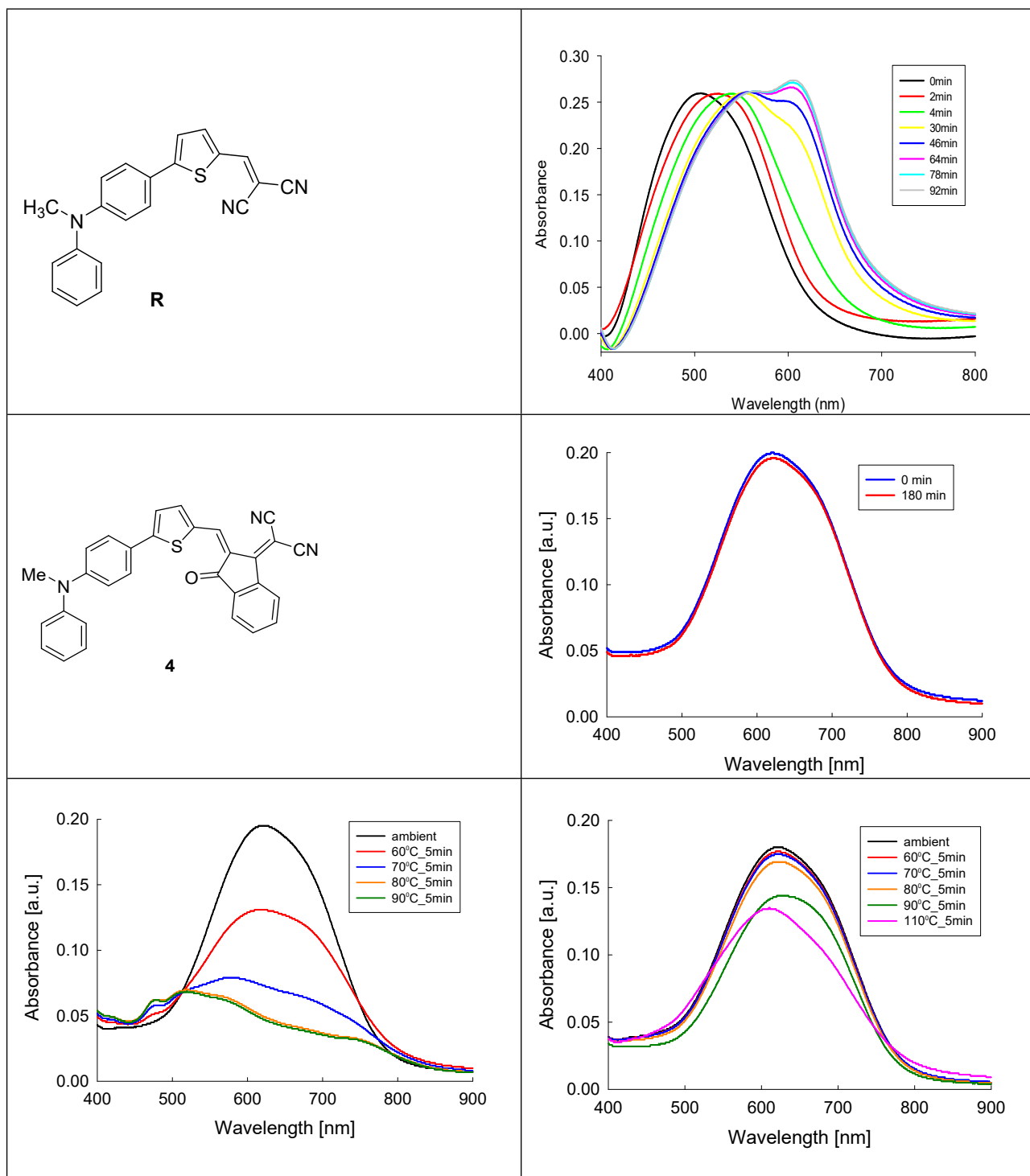


Fig. S8. Top: spontaneous evolution of the optical spectrum of a film of compound **R** at ambient temperature at various time intervals (from J. Mater Chem. 2015, 3, 5145). Middle: Absorption spectra of a film of compound **4** at ambient temperature at various time intervals. Bottom: Absorption spectra of films of compound **4** after heating at various temperature. Left : spun cast film, right: vacuum deposited film. Note the much better stability of vacuum deposited films.

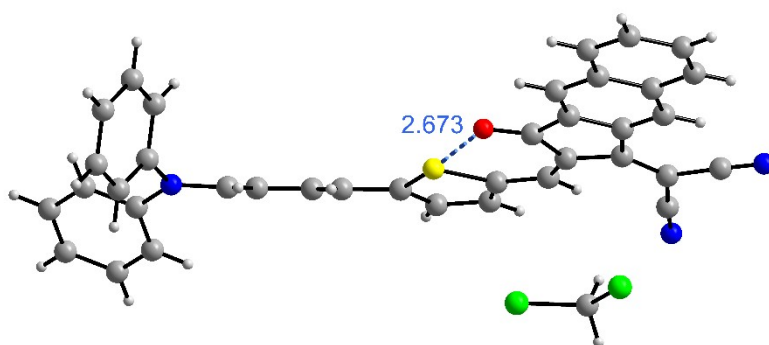


Fig. S9. S...O intramolecular interactions in the crystal structure of compound **6**.

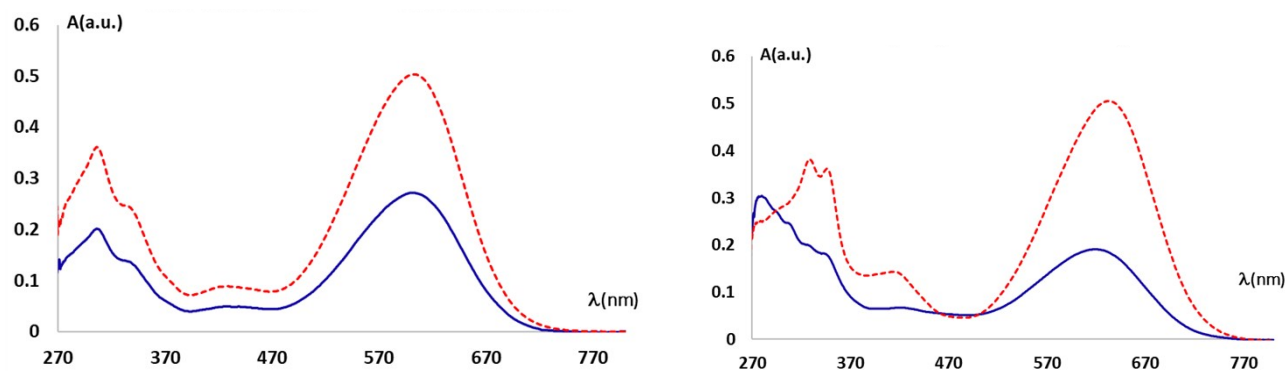


Fig. S10. UV-VIS absorption spectra of compound **3** (left) and **6** (right): dotted line (10mM in DCM), solid line (DCM solution obtained from the redissolution of thermally evaporated films).

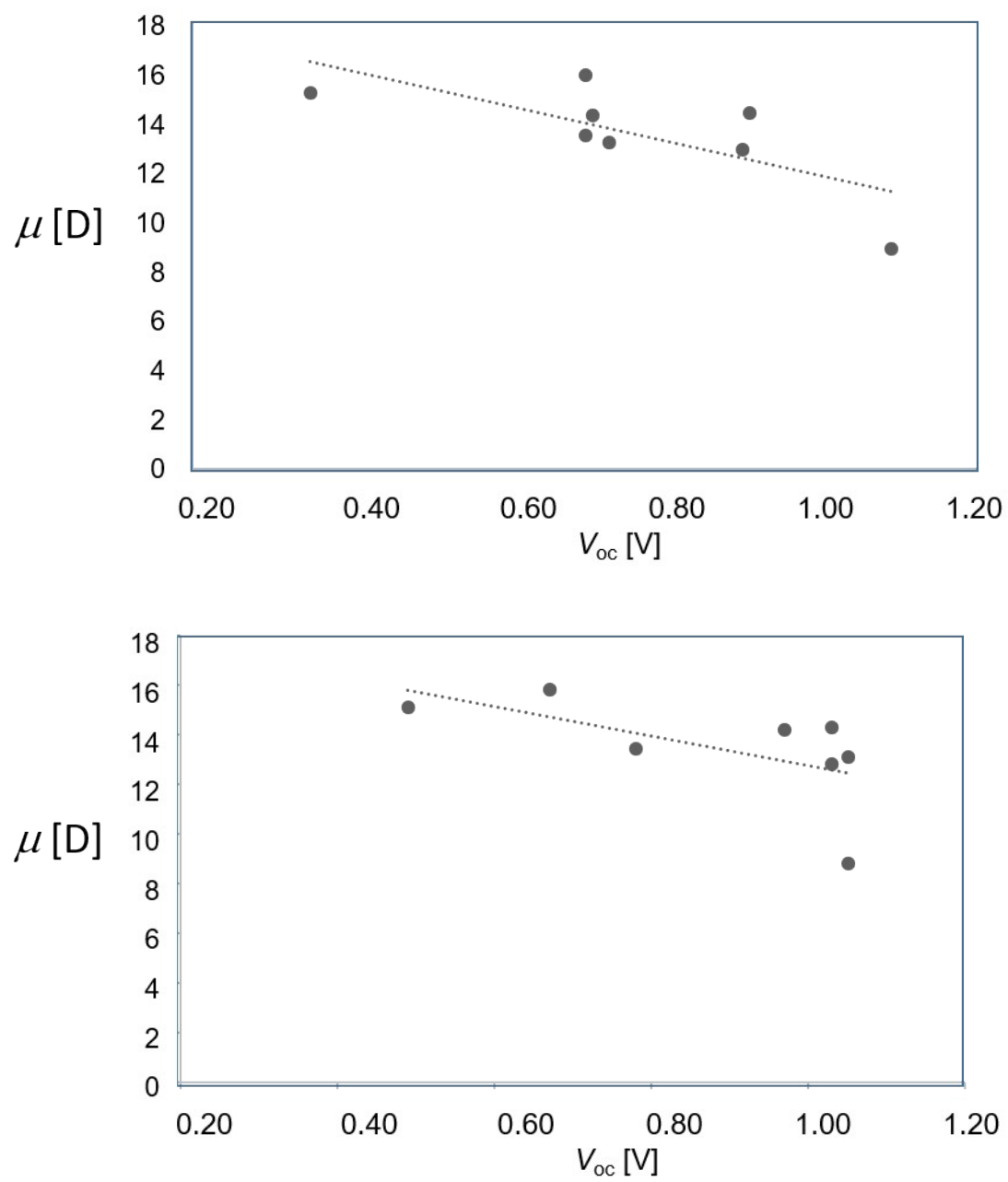


Fig. S11. Variation of V_{oc} vs dipole moment. Top: direct cells, bottom inverted cells

Table S2. Photovoltaic characteristics homo-junction cells based on 1-8 under AM 1.5 simulated solar light with a power light intensity of 100 mW cm⁻².

Compd	J_{sc} [mA cm ⁻²]	V_{oc} [V]	FF [%]	PCE [%]	
1	0.77	0.94	27.76	0.20	
	0.65	0.95	27.92	0.17	
	0.72	0.91	28.01	0.18	
	0.77	0.88	28.12	0.19	
	0.78	0.92	27.94	0.20	
	0.77	0.90	27.96	0.19	
	0.73	0.88	28.10	0.18	
2	0.78	0.68	33.86	0.18	
	0.72	0.67	32.34	0.16	
	0.72	0.73	32.00	0.17	
	0.78	0.79	33.71	0.21	
	0.77	0.72	33.48	0.18	
	0.75	0.64	33.71	0.16	
	0.76	0.74	34.12	0.19	
	0.77	0.69	33.85	0.18	
	0.76	0.78	33.60	0.20	
	0.74	0.70	33.55	0.17	
	0.73	0.73	34.44	0.18	
3	1.49	0.79	39.12	0.46	
	1.82	0.68	33.84	0.42	
	1.76	0.65	33.46	0.38	
	1.58	0.69	33.02	0.36	
	1.79	0.74	31.33	0.42	
	1.86	0.72	31.82	0.43	
	1.89	0.71	31.98	0.43	
	1.77	0.70	31.89	0.40	
	1.87	0.72	31.78	0.43	
4	1.28	0.68	39.89	0.35	
	1.26	0.71	37.70	0.34	
	1.25	0.68	39.76	0.34	
	1.23	0.71	37.65	0.33	
	1.13	0.70	37.71	0.30	
	1.28	0.68	39.88	0.35	
	1.17	0.70	37.48	0.31	
	5	1.48	0.90	33.92	0.45
1.56		0.90	33.45	0.47	
1.48		0.90	33.67	0.45	
1.45		0.89	33.69	0.43	
1.54		0.90	33.32	0.46	
1.47		0.89	34.02	0.45	
1.49		0.90	33.59	0.45	
1.57		0.90	33.70	0.47	
6		0.82	0.60	30.56	0.15
		0.80	0.62	30.07	0.15
	0.80	0.68	29.78	0.16	
	0.77	0.66	29.39	0.15	
	0.74	0.65	29.37	0.14	
	0.81	0.63	30.24	0.15	
	0.76	0.66	29.55	0.15	
	0.79	0.70	28.87	0.16	
	0.81	0.60	30.72	0.15	
	0.76	0.67	29.75	0.15	
	7	0.36	0.37	31.23	0.042
0.43		0.34	36.64	0.053	
0.43		0.33	36.62	0.051	
0.40		0.32	36.45	0.047	
0.46		0.35	36.99	0.060	
0.40		0.33	36.51	0.048	
0.39		0.39	30.82	0.046	
0.39		0.35	37.09	0.052	
0.46		0.36	37.00	0.061	
8		0.99	1.09	29.86	0.32
	0.92	1.07	29.41	0.29	
	0.94	1.07	30.51	0.31	
	0.94	1.10	29.28	0.30	
	0.90	1.10	28.58	0.28	
	0.89	1.08	29.82	0.29	
	0.99	1.09	30.15	0.33	
	0.89	1.08	29.11	0.28	
	1.00	1.11	29.36	0.32	
	0.88	1.08	29.42	0.28	

Table S3. Photovoltaic characteristics for p-i-n cells based on **1-8** under AM 1.5 simulated solar light with a power light intensity of 100 mW cm⁻².

Compd	J_{sc} [mA cm ⁻²]	V_{oc} [V]	FF [%]	PCE [%]	
1	1.80	1.02	28.43	0.52	
	1.79	0.92	28.22	0.46	
	1.86	1.03	28.91	0.55	
	1.85	0.91	28.88	0.49	
	1.82	1.07	28.24	0.55	
	1.71	0.94	29.39	0.47	
	1.73	0.97	28.96	0.49	
	1.60	0.98	28.97	0.46	
	1.71	0.94	29.39	0.47	
	1.72	0.77	32.42	0.43	
	1.59	0.88	29.22	0.41	
2	1.52	0.79	31.59	0.38	
	1.55	0.81	31.49	0.39	
	1.66	0.84	31.03	0.43	
	1.65	0.79	31.03	0.41	
	1.41	0.83	31.14	0.36	
	1.66	0.86	30.73	0.44	
	1.60	0.78	30.47	0.38	
	1.63	0.94	29.91	0.46	
	1.52	0.86	30.68	0.40	
	1.66	0.97	30.71	0.49	
	3.41	1.05	23.60	0.84	
3	3.47	1.05	23.54	0.85	
	3.37	1.04	23.66	0.83	
	3.29	1.05	23.50	0.81	
	3.09	1.04	23.68	0.76	
	3.34	1.05	23.51	0.82	
	3.49	1.04	23.75	0.86	
	3.36	1.04	23.63	0.83	
	3.32	1.06	23.30	0.82	
	3.36	1.04	23.70	0.83	
	3.14	1.04	24.00	0.78	
	3.32	1.04	23.94	0.83	
3.09	1.04	23.58	0.75		
3.22	1.05	23.85	0.81		
3.42	1.05	23.72	0.85		
2.17	1.09	24.03	0.57		
2.05	1.06	24.37	0.53		
1.84	1.05	24.51	0.47		
1.92	1.11	23.58	0.50		
2.13	1.00	24.99	0.54		
4	2.47	0.66	31.10	0.51	
	2.69	0.62	31.20	0.52	
	2.47	0.66	31.10	0.51	
	2.60	0.72	28.78	0.54	
	2.62	0.67	31.31	0.55	
	2.40	0.67	31.42	0.51	
	2.52	0.70	31.66	0.56	
	2.61	0.70	31.55	0.58	
	2.57	0.67	31.84	0.54	
	2.14	0.69	32.74	0.48	
	2.56	0.62	34.45	0.55	
5	2.32	0.67	31.59	0.49	
	2.44	0.68	31.92	0.53	
	3.47	1.03	24.02	0.85	
	3.50	1.03	23.93	0.87	
	3.17	1.03	24.08	0.78	
	3.32	1.04	23.93	0.82	
	3.34	1.03	23.86	0.82	
	3.50	1.04	23.83	0.87	
	3.42	1.04	23.79	0.84	
	3.42	1.03	24.21	0.85	
	3.29	1.03	24.44	0.82	
3.37	1.04	24.20	0.85		
3.14	1.03	24.46	0.80		
2.22	0.66	27.45	0.41		
6	1.99	0.71	27.42	0.39	
	2.23	0.69	27.27	0.42	
	2.37	0.78	26.51	0.49	
	2.41	0.69	27.28	0.45	
	2.34	0.68	27.62	0.44	
	1.84	0.75	27.01	0.37	
	2.22	0.72	26.54	0.43	
	1.94	0.71	26.39	0.37	
	2.25	0.74	26.93	0.45	
	7	0.71	0.49	25.67	0.090
		0.73	0.54	25.38	0.100
0.71		0.43	27.20	0.083	
0.72		0.45	26.67	0.086	
0.73		0.54	25.53	0.101	
0.71		0.48	25.96	0.088	
0.72		0.52	25.24	0.095	
0.72		0.46	25.01	0.083	
0.75		0.54	25.45	0.103	
0.72		0.42	27.02	0.081	
2.15		1.05	23.83	0.54	
8	2.18	0.90	26.56	0.52	
	2.11	1.10	22.77	0.53	
	2.17	1.09	24.03	0.57	
	2.05	1.06	24.37	0.53	
	1.84	1.05	24.51	0.47	
	1.92	1.11	23.58	0.50	
	2.13	1.00	24.99	0.54	
	2.08	1.11	23.28	0.54	
	1.83	1.09	23.97	0.48	
	1.90	1.06	24.33	0.49	
	2.00	1.00	25.36	0.51	

1. G. M. Sheldrick, *Acta Crystallogr., Sect. C: Struct. Chem.* **2015**, *C71*, 3.
2. M. J. Frisch, G. W. Trucks, H. B. Schlegel, G. E. Scuseria, M. A. Robb, J. R. Cheeseman, G. Scalmani, V. Barone, B. Mennucci, G. A. Petersson, et al., Gaussian 09, revision E.01, Gaussian, Inc., Wallingford, CT, 2009.
3. S. Grimme, J. Antony, S. Ehrlich and H. Krieg, *J. Chem. Phys.*, **2010**, *132*, 154104.
4. A. Schafer, C. Huber and R. Ahlrichs, *J. Chem. Phys.*, **1994**, *100*, 5829.
5. D. Rappoport and F. Furche, *J. Chem. Phys.*, **2010**, *133*, 134105.